We express our sincere gratitude to the Editor and the two referees for their insightful and constructive comments. Please find below our point-by-point replies. All the comments are presented in black text and the corresponding replies are highlighted in blue.

## Referee #1

The authors use a fully coupled climate model to evaluate the response of permafrost under temperature stabilization and overshoot scenarios. The methods appear rigorous, and the manuscript is well-written. However, the manuscript could be improved by discussing the implications of some of the feedbacks being modeled. Substantial revisions to some sections of the text and figures could further improve the overall clarity of the manuscript and link it more directly to existing literature.

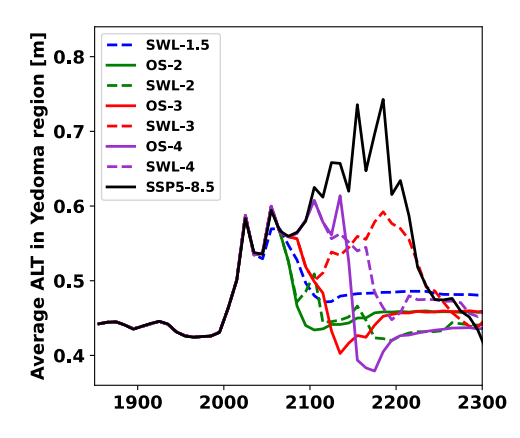
## Major comments:

Line 92 and throughout: Yedoma represents a significant, deep proportion of the permafrost carbon stock in some regions and was formed over extremely long timescales. Given the focus on differences between overshoot and stabilization scenarios, a greater discussion of this limitation could be included in the methods and conclusions.

We appreciate your insightful comment. The UVic ESCM v2.10 simulates permafrost carbon only in the top six layers (to a depth of 3.35 m), and therefore omits soil carbon stored in the deep deposits of Yedoma regions. As a result, we cannot directly estimate the impacts of temperature overshoot on deep Yedoma carbon, or compare these changes relative to stabilization scenarios. To address this limitation, we analyzed the average and maximum active layer thickness (ALT) in Yedoma regions between the overshoot and stabilization scenarios simulated in this study. Using differences in ALT as a proxy to infer the potential impacts on deep Yedoma carbon (Figure S6). To clarify this point, we have added the following paragraph to Section "4 Conclusions and Discussion":

"This study does not simulate the changes of deep Yedoma carbon under the temperature stabilization and overshoot scenarios. Yedoma deposits represent a significant deep carbon reservoir and are widespread across Siberia, Alaska, and the Yukon region of Canada, having primarily formed during the late Pleistocene, especially in the late glacial period. These deep, perennially frozen sediments are particularly ice-rich, and the freeze-locked organic matter in such deposits can be re-mobilized on short time-scales, representing one of the most vulnerable permafrost carbon pools under future warming scenarios (Schuur et al., 2015; Strauss et al., 2017). According to Zimov et al. (2006), these perennially frozen Yedoma sediments cover more than 1 million km<sup>2</sup>, with an average depth of approximately 25 m. Recent estimates place the organic carbon stock in Yedoma deposits at  $213 \pm 24$  PgC, constituting a significant portion of the total permafrost carbon pool (Strauss et al., 2017). However, the UVic ESCM v2.10 utilized in this study simulates permafrost carbon only within the top 3.35 m of soil, limiting our ability to directly assess the impacts of temperature overshoot on deep Yedoma carbon. Considering their ice-rich nature and potential susceptibility to rapid-thaw processes, we analyzed the average and maximum active layer thickness (ALT) in Yedoma regions (Strauss et al., 2021, 2022) under the simulated scenarios to approximate potential impacts. We find that the average ALT in Yedoma regions remains below 1 m in all stabilization and overshoot scenarios, while the maximum ALT rarely exceeds 3.35 m in overshoot

scenarios but does exceed this depth in some stabilization scenarios. However, in all scenarios, the maximum ALT does not exceed 6 m, which is relatively shallow compared to the average depth (~25 m) of Yedoma deposits (Figure S6). Consequently, the impact on Yedoma is considered to be minimal in all scenarios, and the effect of overshoot scenarios on the deep Yedoma carbon is relatively minor compared to stabilization scenarios as well."



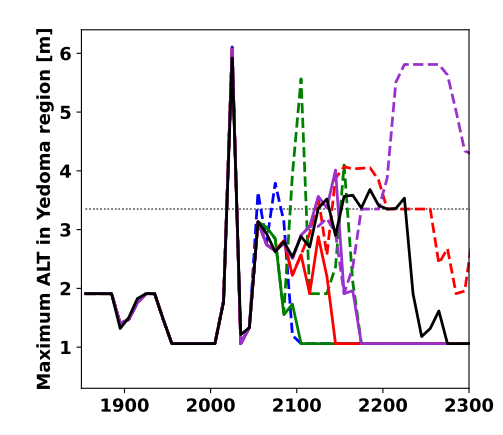


Figure S6. Timeseries of annual (a) average and (b) maximum active layer thickness (ALT) in Yedoma regions under overshoot (colored solid lines) and stabilization (colored dashed lines) scenarios at 1.5 °C (blue), 2.0 °C (green), 3.0 °C (red), and 4.0 °C (purple) GWLs, as well as the SSP5-8.5 scenario (black solid line). Results represent the ensemble median of 250 simulations based on the PFC simulations. The Yedoma region mask used in this analysis is based on the Ice-Rich Yedoma Permafrost Database Version 2 (IRYP v2) (Strauss et al., 2021, 2022; https://doi.org/10.1594/PANGAEA.940078).

Line 90 - 103: More background on the UVICC ESM permafrost carbon model, validation, and perturbed parameter approach would be particularly useful to readers.

Thank you for your valuable suggestion. To improve clarity and provide a more comprehensive background, we have made the following revisions to Section "2.1 Model description":

"The UVic ESCM v2.10 represents the terrestrial subsurface with 14 layers, extending to a total depth of 250.3 m to correctly capture the transient response of permafrost on centennial timescales. The top eight layers (10.0 m) are involved in the hydraulic cycle, while the deeper layers are modeled as impermeable bedrock (Avis et al., 2011). The carbon cycle is active in the top six layers (3.35 m), where organic carbon from litterfall, simulated by the TRIFFID vegetation model, is allocated to soil layers with temperatures above 1 °C according to an exponentially decreasing function with depth. If all soil layers are below 1 °C, the organic carbon is added to the top soil layer. The soil respiration is calculated for each layer individually as a function of temperature and moisture, but the respiration ceases when the soil layer temperature falls below 0 °C (Meissner et al., 2003; Mengis et al., 2020). In regions where permafrost exists—defined as areas where soil temperature remains below 0 °C for at least two consecutive years—the model applies a revised diffusion-based cryoturbation scheme to redistribute soil carbon within the soil column. Compared to the original diffusion-based cryoturbation scheme proposed by Koven et al. (2009), the revised cryoturbation scheme calculates carbon diffusion using an effective carbon concentration that

incorporates the volumetric porosity of the soil layer, rather than the actual carbon concentration, thereby resolving the disequilibrium problem of the permafrost carbon pool during model spin-up (MacDougall and Knutti, 2016). However, as the UVic ESCM v2.10 only simulates permafrost carbon in the top 3.35 m of soil, the current cryoturbation scheme cannot initiate the formation of Yedoma. As a result, soil carbon stored in deep deposits of Yedoma regions is omitted in our simulations."

The perturbed parameter approach is described at the end of Section "2.2 Experimental Design". We have refined the description to improve coherence. Additionally, we have added a figure to illustrate the probability distribution functions of the four perturbed key permafrost carbon parameters (Figure 2). The revised text and added figure are as follows:

"The Latin hypercube sampling method (McKay et al., 1979) was used to explore the effects of parameter uncertainty on projections of permafrost carbon change. In this study, the probability distribution function of each key permafrost carbon parameter was divided into 25 intervals of equal probability. One value was randomly selected from each interval for a given parameter, and then randomly matched with values of the other three key parameters selected in the same manner to generate parameter sets. This sampling procedure was repeated 10 times, resulting in 250 unique parameter sets (i.e., 250 model variants). For each parameter set, the UVic ESCM v2.10 was first run through a 10,000-year spin-up phase under pre-industrial conditions to achieve a quasi-equilibrium state. For these spin-up runs, the atmospheric CO<sub>2</sub> concentration was fixed at 284.7 ppm and the solar constant was set to 1360.747 W m<sup>-2</sup>. Following the spin-up, emission-driven transient experiments were conducted under the stabilization, overshoot and SSP5-8.5 scenarios. The results are presented as the median across all model variants, with uncertainty quantified as the range between the 5th to the 95th percentiles."

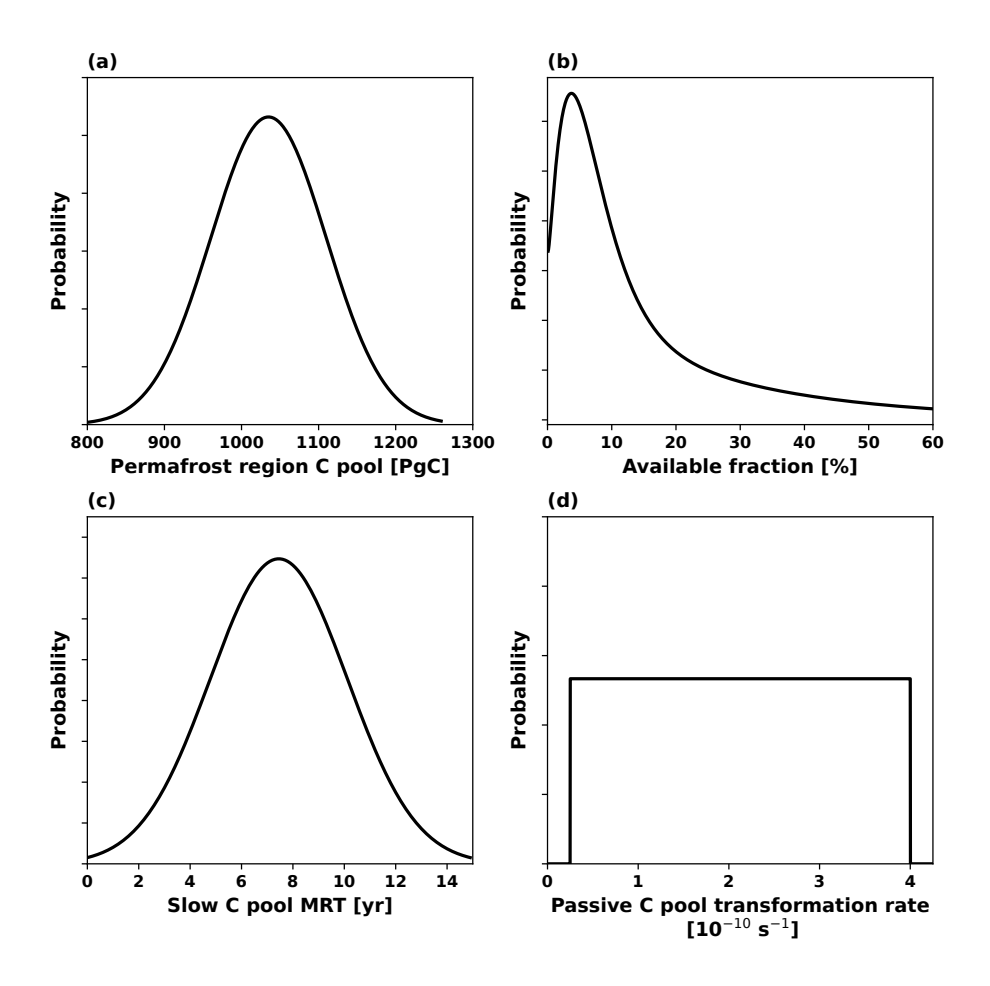


Figure 2. Probability distribution functions of the four key permafrost carbon parameters perturbed in the UVic ESCM v2.10 to represent uncertainty in permafrost carbon response. Panel (d) employs a logarithmic scale on the horizontal axis to better illustrate the distribution of the corresponding parameter. This figure is reproduced from MacDougall (2021).

Model validation has been incorporated into the first paragraph in Section "3 Results". The added content is:

"The UVic ESCM v2.10 reliably simulates historical temperature changes, permafrost area, and the partitioning of anthropogenic carbon emissions among the atmosphere, ocean and land. Under preindustrial conditions, the simulated Northern Hemisphere permafrost area, defined as regions where the soil layer remains perennially frozen for at least two consecutive years, was 17.01 [17.00 to 17.04] million km², the simulated total soil carbon stock in the permafrost regions was 1031 [915 to 1149] PgC, of which 484 [383 to 590] PgC was classified as perennially frozen carbon and 547 [533 to 559] PgC was classified as usual soil carbon. During For the period 1960–1990, the model simulated Northern Hemisphere permafrost area at 16.8 [16.7 to 16.9] million km², which falls within the reconstructed range from 12.0 to 18.2 million km² (Chadburn et al., 2017) and the observation derived extent from 12.21 to 16.98 million km² (Zhang et al., 2000). Additionally, the simulated soil carbon stock in the top 3.35 m of permafrost regions for this same period was 1034 [919 to 1151] PgC, with 483 [382 to 587] PgC classified as perennially frozen carbon, accounting for 47% [42% to 51%] of the total permafrost soil carbon stock, in agreement with Hugelius et al. (2014). During the period 2011–2020, the model estimated a global mean temperature increase of

1.14 [1.13 to 1.15] °C relative to preindustrial levels, which is closely aligned with the observed rise of 1.09 [0.91 to 1.23] °C (Gulev et al., 2021). From 2010 to 2019, the model estimated that anthropogenic carbon emissions were distributed as follows: 5.5 [5.4 to 5.6] PgC yr<sup>-1</sup> to the atmosphere, 3.0 [2.98 to 3.03] PgC yr<sup>-1</sup> to the ocean, and 2.5 [2.4 to 2.6] PgC yr<sup>-1</sup> to terrestrial ecosystems. These estimates are broadly consistent with the global anthropogenic CO<sub>2</sub> budget assessment by the Global Carbon Project (GCP) with figures of 5.1±0.02 PgC yr<sup>-1</sup> for the atmosphere, 2.5±0.6 PgC yr<sup>-1</sup> for the ocean, and 3.4±0.9 PgC yr<sup>-1</sup> for terrestrial ecosystems (Friedlingstein et al., 2020)."

Line 129 – 136: More clarity is needed about this aspect of the method and the interaction with any permafrost feedback loops. It appears these experiments were done to create drivers for the overshoot scenarios (i.e. the proportional control scheme is not active when the final model runs for analysis are done). It then appears based on this text and the text in section 3.2 that any permafrost carbon fluxes would be tacked onto the emissions and removals needed to accomplish these scenarios. Significant edits are needed here for clarity. The additional warming in Figure 5 also appears well-suited for additional discussion.

Thank you for your detailed comments. Actually, the proportional control scheme was used only in the initial set of simulations, which were conducted to generate CO<sub>2</sub> emission trajectories that follow the intended warming pathways of each scenario (Fig. 1a). These emission trajectories were then used to drive the formal experiments for both stabilization and overshoot scenarios, without any further application of the proportional control scheme during the final model integrations.

To isolate the contribution of permafrost carbon feedback, we conducted two parallel sets of formal experiments for each scenario, both driven by the same CO<sub>2</sub> emission trajectories. The only difference between these sets lies in whether the permafrost carbon module was activated or not. As you noted, any permafrost carbon fluxes would be tacked onto the emissions and removals needed to accomplish these scenarios. To clearly distinguish the role of permafrost carbon feedback, we refer to the simulations with the permafrost carbon module activated as PFC simulations, and those with the module deactivated as NPFC simulations. The comparison between the PFC and NPFC simulations allows us to robustly isolate the additional warming and radiative forcing induced by permafrost carbon emissions under both stabilization and overshoot scenarios.

To improve clarity, we have revised the relevant section as follows:

"To isolate the contribution of permafrost carbon feedback, two parallel sets of formal experiments were conducted for each scenario, both driven by the same CO<sub>2</sub> emission trajectories diagnosed from the initial simulations. One set activated the permafrost carbon module and is referred to as PFC simulations, while the other set deactivated the permafrost carbon module and is referred to as NPFC simulations. Since the emissions trajectories were diagnosed from the initial simulations in which the proportional control scheme was applied to achieve the desired temperature pathways, applying them in the formal simulations with the permafrost carbon module deactivated can effectively achieve the designed temperature trajectories (Fig. 1b). However, applying the diagnosed emissions in simulations with the permafrost module activated results in any permafrost carbon fluxes being effectively added on top of the diagnosed emissions, thereby causing additional

warming. In other words, to achieve the intended climate targets under the same emission pathways, removals equivalent to the permafrost carbon emissions would be required. Therefore, the comparison between the PFC and NPFC simulation sets provides a robust framework to isolate and quantify the additional warming and radiative forcing effects due to permafrost carbon emissions under stabilization and overshoot scenarios. For comparison, two parallel simulations with permafrost carbon module activated or deactivated were also conducted for the high-emissions SSP5-8.5 scenario."

We have also revised the first paragraph of Section "3.2 Radiative Impacts of Permafrost Carbon Release" on radiative impacts of permafrost carbon release to better clarify the expression of additional warming. The revised text is as follows:

"The permafrost carbon release would increase global mean radiative forcing and surface temperature. By comparing two parallel sets of simulations with the permafrost carbon module activated (PFC) or deactivated (NPFC), we were able to quantify the additional radiative forcing and warming caused by permafrost carbon release."

In Section "4 Conclusions and Discussion", we have added a paragraph on the additional warming caused by the permafrost carbon release and its implications on CO<sub>2</sub> emission budgets, as follows:

"Different permafrost carbon release and associated additional warming under overshoot scenarios confirm the path-dependent fate of permafrost region carbon (Kleinen and Brovkin, 2018) and the path-dependent reductions in CO<sub>2</sub> emission budgets (MacDougall et al., 2015; Gasser et al., 2018). As the permafrost carbon was accumulated very slowly during the last millions of years, its release would be tacked onto the anthropogenic CO<sub>2</sub> emissions, and the resulting additional warming poses a challenge to achieving global climate goals by substantially reducing the remaining carbon budget compatible with the Paris Agreement (MacDougall et al., 2015; Natali et al., 2021). In the overshoot scenarios simulated in this study, permafrost carbon release by 2300 ranges from 60 [35 to 87] PgC to 97 [63 to 135] PgC. The associated additional warming caused by the release ranges from 0.10 [0.06 to 0.15] °C to 0.18 [0.11 to 0.25] °C. This permafrost carbon feedback contributes a substantial addition on top of 1.5 °C warming target under overshoot scenarios, and the magnitude of this additional warming rises with the amplitude of overshoot. To accomplish the 1.5 °C target under the OS-2, OS-3, and OS-4 scenarios, anthropogenic carbon emissions would be reduced by amounts equivalent to the permafrost carbon release. The proportion of carbon removal required to offset permafrost emissions is estimated at 4.9 [2.9 to 7.1] %, 6.5 [4.1 to 9.2] %, and 8.3 [5.4 to 11.6] % by 2300, respectively. Our findings are consistent with previous research utilizing the Monte Carlo ensemble method to evaluate the response of permafrost carbon and its influence on CO<sub>2</sub> emission budgets under overshoot scenarios targeting a 1.5 °C warming limit (Gasser et al., 2018). Specifically, for overshoot amplitudes of 0.5 °C (peak warming of 2 °C) and 1 °C (peak warming of 2.5 °C), the reductions in anthropogenic CO<sub>2</sub> emissions due to permafrost are estimated to be 130 (with a range of 30 - 300) Pg CO<sub>2</sub> and 210 (with a range of 50 - 430) Pg CO<sub>2</sub>, respectively, to meet the long-term 1.5 °C target (Gasser et al., 2018). These results are comparable to our estimates of 60 [35 to 87] PgC under OS-2 and 78 [50 to 111] PgC under OS-3. The differences between the two studies may be partly attributed to different warming trajectories to achieve the same 1.5 °C target. Our study further confirms that if negative CO<sub>2</sub> emissions were to be used to reverse the

anthropogenic climate change, the delayed permafrost carbon release would reduce its effectiveness (MacDougall, 2013; Tokarska and Zickfeld, 2015)."

Line 159 – 169: I appreciate the perturbed parameter approach that's been taken here. It's presented well as uncertainty bounds in the text but includes some cues about the quantity of runs used and uncertainty bounds in more key figures would highlight it. Moreover, I recommend some discussion of any overlapping trajectories given the range of parameter uncertainty. Otherwise, these aspects of the manuscript may not be as apparent to the reader.

Thank you for your valuable suggestion. We have included the uncertainty bounds in the figures showing global warming, permafrost area loss, permafrost carbon loss and permafrost region soil carbon loss (Figure 2 in the original manuscript, Figure 3 in the revised manuscript); changes in permafrost carbon inputs and decomposition, as well as permafrost region soil carbon inputs and decomposition (Figure 4 in the original manuscript, Figure 5 in the revised manuscript); and additional changes in radiative forcing, global warming and permafrost area due to permafrost carbon-climate feedback (Figure 5 in the original manuscript, Figure 7 in the revised manuscript) under overshoot and stabilization scenarios.

To facilitate the discussion of overlapping trajectories of the permafrost carbon, we have expanded the paragraph on the assessment of the relative importance of perturbed model parameters for permafrost region soil carbon release. In addition, we have placed this paragraph in Section "3.1 Permafrost Response" to enhance content coherence. The expanded paragraph reads as follows:

"The uncertainty in permafrost region soil carbon release is nearly the same as that of permafrost carbon release (Fig. 3c, d; Fig. S1c, d). For example, the 5th to 95th percentile range of permafrost region soil carbon release under the OS-2 and OS-4 scenarios is 58 PgC and 81 PgC respectively, compared to 52 PgC and 72 PgC for permafrost carbon release. This indicates that the uncertainty in permafrost region soil carbon release is largely driven by the uncertainty in permafrost carbon release. Therefore, we evaluate the relative importance of perturbed permafrost carbon parameters on permafrost region soil carbon release under different temperature pathways through calculating their correlations across all ensemble simulations. In the SSP5-8.5, OS-4, and SWL-4 scenarios, the influence of model parameters on the uncertainty of permafrost carbon losses by 2300 is relatively consistent, with the strongest correlations observed for the permafrost passive carbon pool transformation rate (R=0.81~0.85), followed by the initial quantity of permafrost region soil carbon (R=0.55~0.61). This finding aligns with Ji et al. (2024), who highlights the critical role of these two parameters in the uncertainty of permafrost region soil carbon loss under temperature overshoot and 1.5 °C warming stabilization scenarios."

We have added a discussion of overlapping trajectories in the relevant quantities and explained the overlaps with the aid of the relative importance of perturbed parameters. The added discussion of the overlapping trajectories reads as follows:

"This study, like previous ones, uncovers considerable uncertainty in projections of permafrost carbon under global warming. The uncertainty represented by perturbed model parameters for each scenario can be interpreted as model uncertainty. We note that model uncertainty in permafrost

carbon release gradually increases with the peak warming level and the duration of overshoot for each scenario (Fig. 3c; Fig. S1c). However, the uncertainty ranges in permafrost carbon release for overshoot and stabilization scenarios with adjacent warming levels, such as OS-2, SWL-1.5 and SWL-2, substantially overlap. This is especially evident in low-level warming scenarios, where the uncertainty in projected permafrost carbon release is mainly driven by model uncertainty due to parameter perturbations, rather than scenario-related uncertainty. Given the significant roles of the permafrost passive carbon pool transformation rate and the initial quantity of permafrost region soil carbon in determining the uncertainty of permafrost region soil carbon release, it is expected that these two parameters contribute significantly to the overlapping uncertainty ranges of permafrost carbon and permafrost region soil carbon losses across different warming levels. Due to the interaction with soil carbon inputs, the overlapping uncertainty in permafrost region soil carbon release tends to differ from that of permafrost carbon release. For example, the uncertainty ranges in permafrost carbon release under OS-4 and SSP5-8.5 scenarios show considerable overlap, but the same does not apply to permafrost region soil carbon release, which results from significant differences in soil carbon inputs under distinct CO<sub>2</sub> fertilization backgrounds. The large overlapping uncertainty in projecting permafrost carbon release under low-level warming scenarios, as shown in this study and in previous research (MacDougall, 2015; MacDougall and Knutti, 2016; Gasser et al., 2018), constitutes a significant challenge in accurately estimating the remaining carbon budgets consistent with temperature goals of the Paris Agreement."

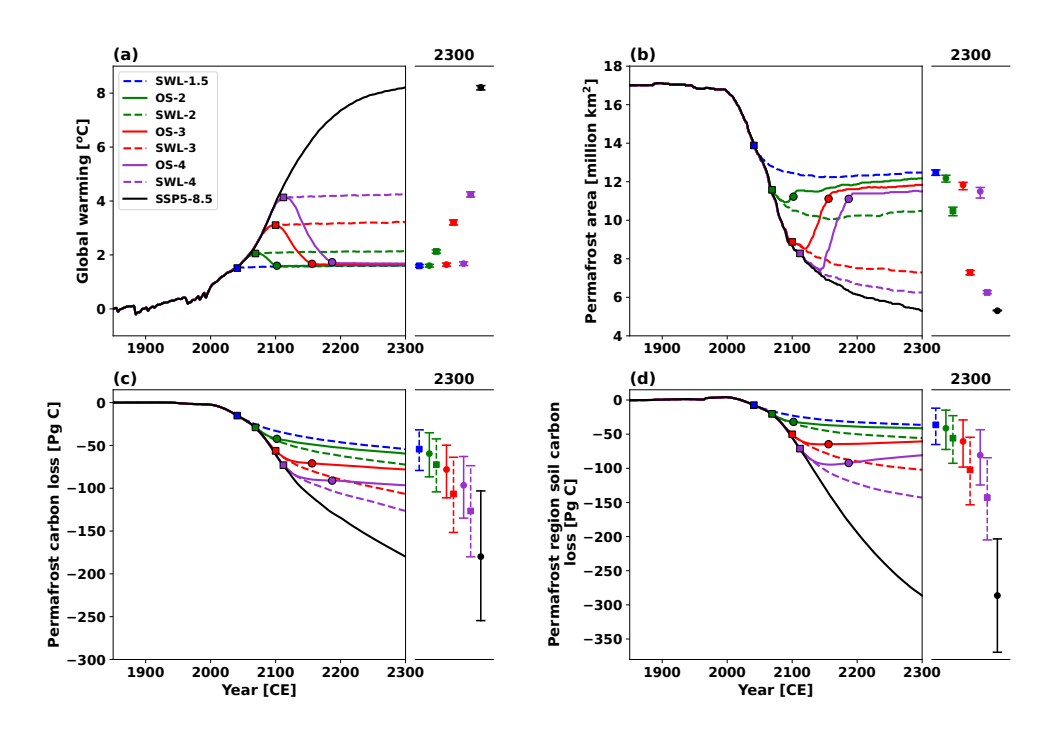


Figure 3. Timeseries of annual mean (a) global warming, (b) permafrost area, (c) permafrost carbon loss and (d) permafrost region soil carbon loss under stabilization (dashed lines) and overshoot (solid lines) scenarios at 1.5 °C (blue), 2.0 °C (green), 3.0 °C (red), and 4.0 °C (purple) global warming levels, as well as the SSP5-8.5 scenario. Square markers indicate the time points when the temperature overshoot reaches its peak or stabilized warming begins, while circle markers indicate when the overshoot returns to 1.5 °C. All changes are relative to the pre-industrial period (1850-1900). Results represent the ensemble median of 250 simulations based on the PFC simulations.

Dots on the right panels represent values in the year 2300, with uncertainty ranges estimated as the 5th to 95th percentiles.

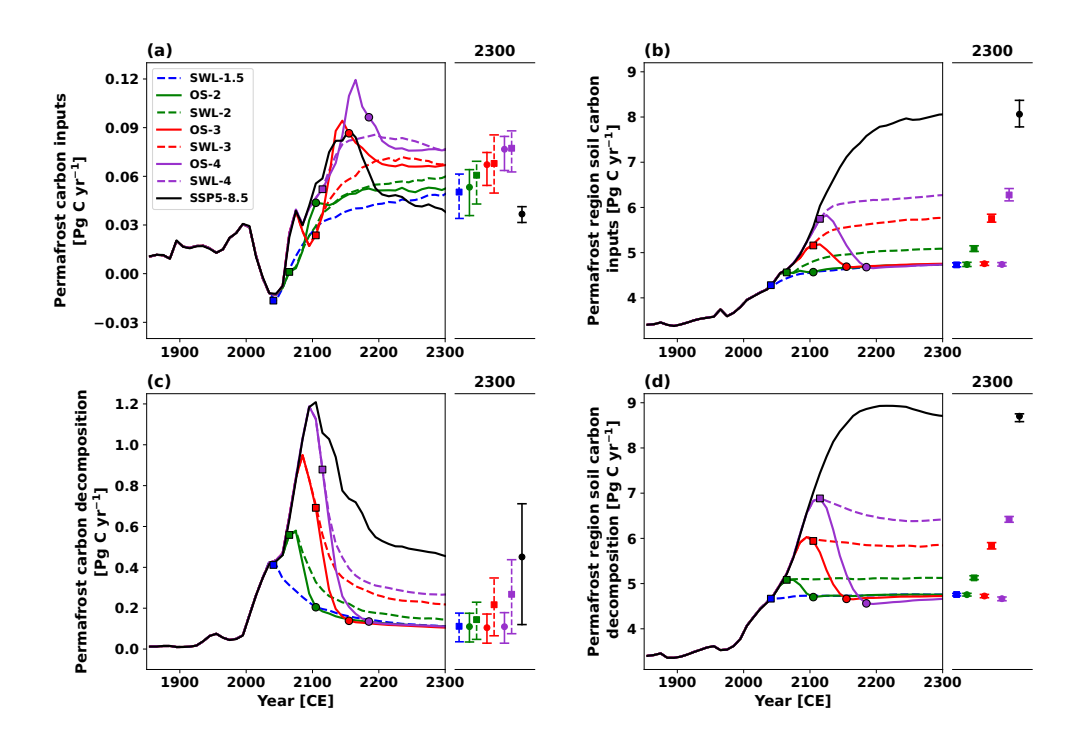


Figure 5. Timeseries of changes in (a) permafrost carbon inputs, (b) permafrost region soil carbon inputs, (c) permafrost carbon decomposition and (d) permafrost region soil carbon decomposition, under the stabilization (dashed lines) and overshoot (solid lines) scenarios at 1.5 °C (blue), 2.0 °C (green), 3.0 °C (red) and 4.0 °C (purple) global warming levels, along with the SSP5-8.5 scenario (black). Square markers indicate the time points when the temperature overshoot reaches its peak or stabilized warming begins, while circle markers indicate when the overshoot returns to 1.5 °C. Results represent the ensemble median of 250 simulations based on the PFC simulations. Dots on the right panels represent values in the year 2300, with uncertainty ranges estimated as the 5th to 95th percentiles.

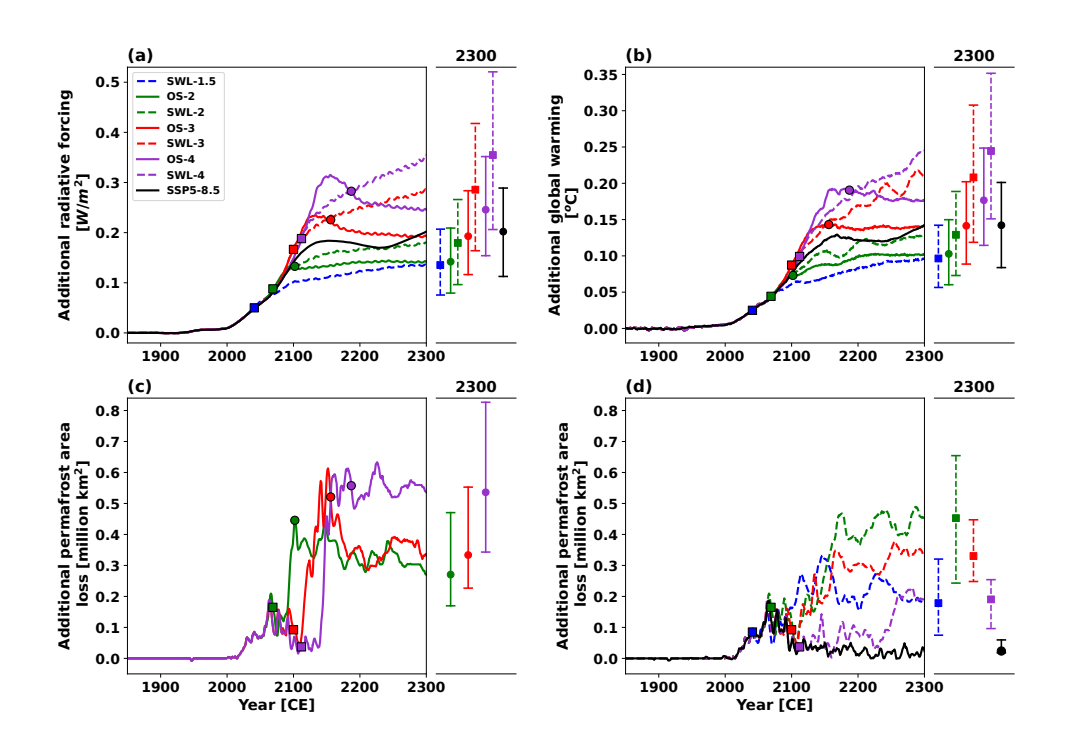


Figure 7. Additional changes in (a) radiative forcing, (b) global warming and (c, d) permafrost area due to permafrost carbon feedback, calculated as the difference between the PFC and NPFC simulations. Shown are results for the stabilization (dashed lines) and overshoot (solid lines) scenarios at 1.5 °C (blue), 2.0 °C (green), 3.0 °C (red) and 4.0 °C (purple) global warming levels, along with the SSP5-8.5 scenario (black). Square markers indicate the time points when the temperature overshoot reaches its peak or stabilized warming begins, while circle markers indicate when the overshoot returns to 1.5 °C. Results represent the ensemble median of 250 simulations. Dots on the right panels represent values in the year 2300, with uncertainty ranges estimated as the 5th to 95th percentiles. In panel (a), the additional radiative forcing is calculated using the simplified expressions (Etminan et al., 2016) based on simulated CO<sub>2</sub> concentrations. In panels (c) and (d), the additional permafrost area loss is smoothed using a 5-year rolling average to eliminate interannual variability.

Line 200: Greater elaboration on this result could be valuable. Assessing this impact at the year 2300 seems reasonable, however, given enough time will all the overshoot scenarios eventually converge with SWL-1.5?

We sincerely appreciate your valuable suggestion. To further investigate whether all overshoot scenarios eventually converge with SWL-1.5, we have extended the SWL-1.5 and overshoot simulations to the year 2400 and compared the permafrost carbon inputs, decomposition and surface climate between them post-overshoot (Figure R1). A new paragraph has been added to Section "4 Conclusions and Discussion" to elaborate on this point and help readers better understand the model's long-term behavior. The added paragraph reads as follows:

"Although permafrost carbon loss is essentially irreversible, overshoot scenarios exhibit a certain degree of recovery relative to the SWL-1.5 stabilization scenario (Fig. 4b; Fig. S2b). It is therefore curious to know whether permafrost carbon under overshoot scenarios will eventually converge

with that under SWL-1.5. Our results show that permafrost carbon inputs are consistently higher under overshoot scenarios than under SWL-1.5, while permafrost carbon decomposition differ only slightly between the two (Fig. 5a, c; Fig. S3a, c). This tends to suggest that the smaller permafrost carbon stocks under overshoot scenarios by 2300 would eventually catch up to the levels under SWL-1.5. To assess this potential convergence, we extended our simulations of both SWL-1.5 and overshoot scenarios to the year 2400 (data not shown). Then we estimated the convergence time by calculating the ratio between the difference in permafrost carbon stocks and the difference in net permafrost carbon inputs (i.e., annual permafrost carbon inputs minus decomposition) for the overshoot scenarios relative to the SWL-1.5 scenario. Based on simulation results for the year 2300, the median estimated convergence times for OS-2, OS-3 and OS-4 are 1076, 1008 and 1433 years, respectively. When using results from the year 2400, the corresponding estimates increase to 1377, 1199 and 1568 years. This means that convergence would take even longer if estimated from later simulation results, mainly due to gradually weakened permafrost carbon inputs. The relatively larger permafrost carbon inputs under overshoot scenarios result mainly from increased litterfall during the overshoot phase. The extra litterfall during the overshoot phase gradually moves through the active layer and is transported to the permafrost zone. Over time, however, the effect of this extra litterfall gradually diminishes, leading to a reduction in permafrost carbon inputs. Consequently, it may take extremely long timescales for the overshoot scenarios to fully converge with SWL-1.5 in terms of permafrost carbon stocks. In addition, due to incomplete recovery of permafrost area and persistent changes in surface climate and soil properties, the overshoot scenarios might ultimately fail to converge to SWL-1.5 scenario in terms of permafrost carbon stocks."

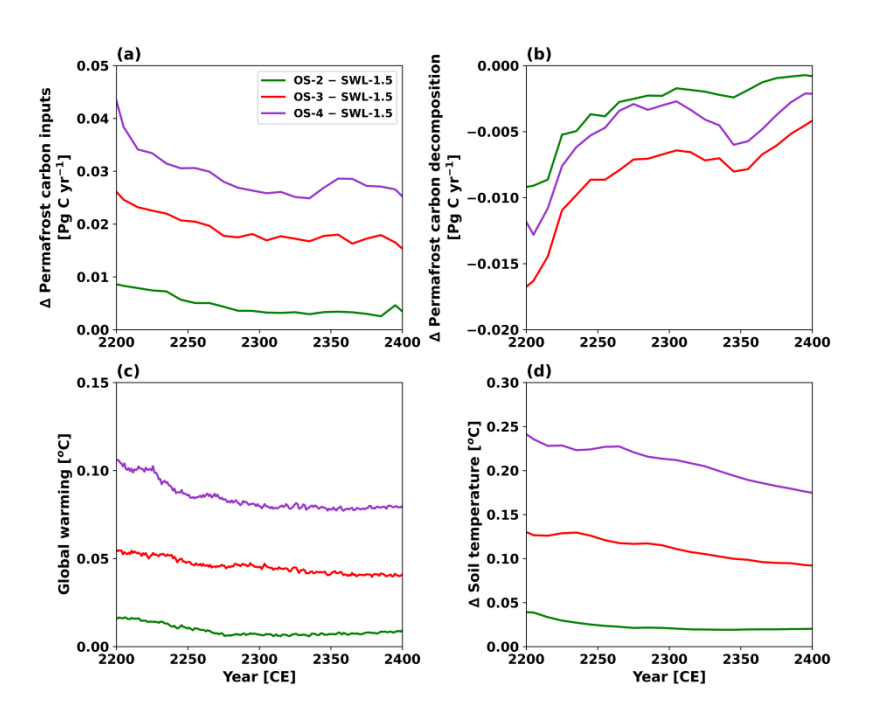


Figure R1. Timeseries of changes relative to the SWL-1.5 scenario in (a) permafrost carbon inputs, (b) permafrost carbon decomposition, (c) global warming and (d) soil temperature in permafrost regions under overshoot scenarios at 2.0 °C (green), 3.0 °C (red), and 4.0 °C (purple) global warming levels from the year 2200 to 2400. Results represent the ensemble median of 250 simulations based on the PFC simulations. Panel (d) shows the regional average of soil temperature in permafrost regions, averaged over the top 3.35 m of soil.

Line 220 and throughout: There is a substantial body of literature related to the response of arctic vegetation to climate change and the processes represented therein. Providing the reader with additional information on the vegetation model within UVICC ESM, the processes represented, limitations therein, including some information about the response of vegetation productivity and framing these results in that context would enhance their presentation. Additional background on the permafrost model would add additional clarity as to why permafrost carbon inputs do not appear to follow the same trajectory as soil carbon.

Thank you for your suggestion. We have expanded the background information on the vegetation model within UVic ESCM as follows in Section "2.1 Model Description":

"The terrestrial component of UVic ESCM v2.10 uses the Top-down Representation of Interactive Foliage and Flora Including Dynamics (TRIFFID) vegetation model to describe the states of five plant functional types (PFT): broadleaf tree, needleleaf tree, C3 grass, C4 grass, and shrub (Cox, 2001; Meissner et al., 2003). A coupled photosynthesis-stomatal conductance model is used to calculate carbon uptake via photosynthesis, which is subsequently allocated to vegetation growth and respiration. The resulting net carbon fluxes drive changes in vegetation characteristics, including areal coverage, leaf area index, and canopy height for each PFT. The UVic ESCM v2.10 utilized in this study does not account for nutrient limitations in the terrestrial carbon cycle, leading to an overestimation of global gross primary productivity and an enhanced capacity of land to take up atmospheric carbon (De Sisto et al., 2023). However, the model reasonably represents the dominant PFTs of C3 grass, shrub and needleleaf tree at northern high latitudes, although it underestimates vegetation carbon density over this area (Mengis et al., 2020)."

We have also added the response of vegetation productivity in Section "3.1 Permafrost Response" to better understanding permafrost region soil carbon inputs as following:

"The permafrost region soil carbon inputs generally track the trajectory of litter flux across the same area, with an approximate delay of 10-20 years (not shown). To attribute the contribution of permafrost region soil carbon inputs, we examined how dominant vegetation types (needleleaf tree, C3 grass and shrub) over the permafrost region adapt to temperature and atmospheric CO2 concentrations in both overshoot and stabilization scenarios (Fig. 6). Needleleaf trees expand slowly and continuously in the permafrost region in both overshoot and stabilization scenarios, whereas that of shrubs closely follows the trajectory of global mean temperature. The combined areal coverage of trees and shrubs is projected to cover about 62% upon 1.5 °C warming relative to preindustrial levels around 2040s, slightly higher than the 24~52% range projected for 2050 using a statistical approach that links climate conditions to vegetation types under two distinct emission trajectories (Pearson et al., 2013). During the warming and cooling phases of overshoot scenarios, the expansion and reduction of shrubs correspond with the degradation and expansion of C3 grasses, respectively. Among the three dominant PFTs, only shrubs show a nearly reversible response in areal coverage, net primary productivity (NPP) and vegetation carbon with respect to global mean temperature under overshoot scenarios. In contrast, the continuous reduction of C3 grasses and the expansion of needleleaf trees suggest a degree of irreversibility in the structure and vegetation carbon density of northern high latitude terrestrial ecosystems under overshoot scenarios. Our results are in line with an earlier study by Tokarska and Zickfeld (2015), but contrast with Schwinger

et al. (2022) who reported only minor differences in vegetation carbon after the overshoots compared to the reference simulation with no overshoot by prescribing vegetation distributions. In our study, the shifts in vegetation composition and changes in living biomass, especially those associated with woody vegetation, are key drivers of permafrost region soil carbon inputs."

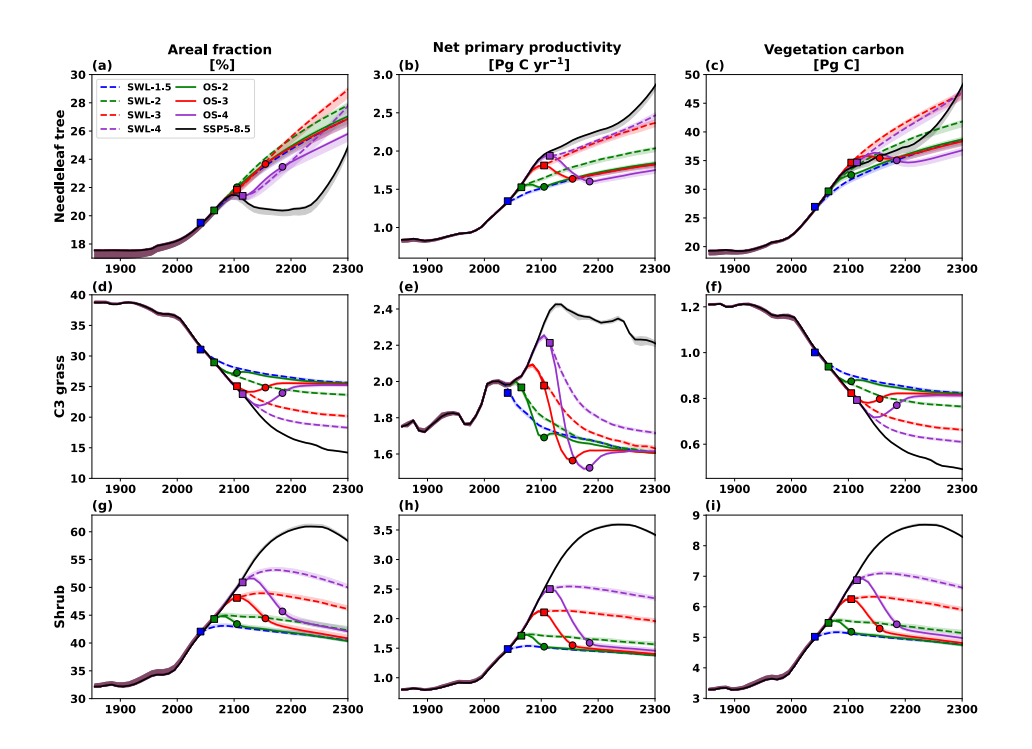


Figure 6. Timeseries of annual mean areal fraction (left column), net primary productivity (middle column) and vegetation carbon (right column) under stabilization (dashed lines) and overshoot (solid lines) scenarios at 1.5 °C (blue), 2.0 °C (green), 3.0 °C (red), and 4.0 °C (purple) global warming levels, as well as the SSP5-8.5 scenario (black). Each row represents one of the three dominant plant functional type (PFT): (a-c) needleleaf tree, (d-f) C3 grass and (g-i) shrub. Square markers indicate the time points when the temperature overshoot reaches its peak or stabilized warming begins, while circle markers indicate when the overshoot returns to 1.5 °C. Results represent the ensemble median of 250 simulations based on the PFC simulations, and the shadings denote the 5th and 95th percentile uncertainty ranges.

To explain why permafrost carbon inputs do not follow the same trajectory as soil carbon, especially under overshoot scenarios, we added the following paragraph in Section "3.1 Permafrost Response":

"Our simulations show that permafrost carbon inputs do not follow the same trajectory as soil carbon, especially under overshoot scenarios. This is likely due to inaccurate parameterization adopted in the current model. As noted in the model description (Section 2.1), litterfall is allocated to soil layers with temperatures above 1 °C according to an exponentially decreasing function of depth. When all soil layers are below 1 °C, organic carbon from the litterfall is added to the top soil layer. Meanwhile, permafrost carbon and non-permafrost soil carbon are both represented as depth-resolved carbon pools within the top six soil layers. The movement of permafrost carbon due to cryoturbation mixing is parameterized as being proportional to the gradient of total soil carbon with depth. Soil carbon that diffuses downward through the permafrost table is converted to permafrost carbon. During the

cooling phase of overshoot scenarios, increased litterfall and a rising permafrost table lead to elevated carbon concentrations in surface soil layers, resulting in enhanced vertical diffusion and a surge in permafrost carbon inputs. Conversely, under the SSP5-8.5 scenario, permafrost carbon inputs exhibit only a minor peak around the 2150s, followed by a sharp decline (Fig. 5a; Fig. S3a). This is due to the continuous reduction in permafrost area and the deepening of the permafrost table, both of which reduce carbon concentrations in the upper soil layers and weaken vertical diffusion, despite the increasing litter flux under a strong CO<sub>2</sub> fertilization background. We note that the approach adopted in the model may not accurately reflect natural processes of vertical carbon movement, which are influenced by soil porosity heterogeneity, freeze-thaw cycles, and ice expansion upon freezing."

## Minor comments:

Abstract: for clarity suggest reducing the use of acronyms in the abstract and possibly parts of the text.

Thank you for your suggestion. In response to your suggestion, we have reduced the use of acronyms in the abstract and replaced "SWL" and "OS" with their full terms, "stabilization" and "overshoot." We will continue to review acronym usage throughout the manuscript to ensure clarity and accessibility.

Line 25: gradual and abrupt seem to refer to the rate of carbon loss suggest revision to distinguish this from the processes of gradual and abrupt thaw.

Thank you for your suggestion. We have revised the wording to ensure that gradual and abrupt explicitly refer to the thawing processes. The sentence has been changed to "gradual or abrupt permafrost thaw, along with subsequent microbial decomposition, would release carbon dioxide (CO<sub>2</sub>) and methane (CH<sub>4</sub>) into the atmosphere...".

Line 50: suggest adding further discission of the mechanism behind the presence or absence of hysteresis behavior in different processes as this is useful background.

Thank you for this insightful suggestion. We agree that a more detailed discussion of the mechanism behind the presence or absence of hysteresis behavior in different processes would strengthen the background of our study. To address this, we have expanded the discussion in this section by highlighting key factors influencing hysteresis in permafrost carbon dynamics, including thermophysical inertia, microbial decomposition lag, and hydrological feedbacks.

The revised text now reads: "The presence or absence of hysteresis effect in the permafrost processes is influenced by multiple factors, including the thermal inertia of permafrost soils, potential shifts in vegetation composition, and the extent to which irreversible permafrost carbon losses are offset by gains in vegetation and non-permafrost soil carbon reservoirs (MacDougall, 2013; Schwinger et al., 2022). Furthermore, the soil carbon loss under overshoot scenarios

significantly affects the hydrological and thermal properties of soils (Zhu et al., 2019), which in turn modulate the processes involved. The interactions between physical and biophysical processes can potentially stabilize the carbon, water, and energy cycles at distinct post-overshoot equilibria (de Vrese and Brovkin, 2021). Therefore, a temporary warming of the permafrost regions entails important legacy effects and lasting impacts on its physical state and carbon cycle."

Line 229: Suggest clarifying the timescale being discussed in this summary information. It reads very similarly to the sentence immediately prior.

Thank you for the suggestion. We have revised this section to improve clarity and to specify the timescale. The revised manuscript is as follows:

"Notably, in all stabilization and overshoot scenarios simulated in this study, the permafrost region soil serves as a net carbon source for atmospheric CO<sub>2</sub> by 2300. However, during the stabilization phase of OS-3 and OS-4, the permafrost region soil turns into a carbon sink, as soil carbon inputs surpass the reduced decomposition activity due to the depletion of soil carbon stocks and reduced warming levels."

## References

Avis, C. A., Weaver, A. J., and Meissner, K. J.: Reduction in areal extent of high-latitude wetlands in response to permafrost thaw, Nature Geoscience, 4, 444–448, https://doi.org/10.1038/ngeo1160, 2011.

Chadburn, S. E., Burke, E. J., Cox, P. M., Friedlingstein, P., Hugelius, G., and Westermann, S.: An observation-based constraint on permafrost loss as a function of global warming, Nature Climate Change, 7, 340 – 344, https://doi.org/10.1038/nclimate3262, 2017.

Cox, P.: Description of the TRIFFID dynamic global vegetation model. Hadley Centre Technical., 24, 1 - 16, 2001.

De Sisto, M. L., MacDougall, A. H., Mengis, N., and Antoniello, S.: Modelling the terrestrial nitrogen and phosphorus cycle in the UVic ESCM, Geoscientific Model Development, 16, 4113 – 4136, https://doi.org/10.5194/gmd-16-4113-2023, 2023.

De Vrese, P. and Brovkin, V.: Timescales of the permafrost carbon cycle and legacy effects of temperature overshoot scenarios, Nature Communications, 12, 2688, https://doi.org/10.1038/s41467-021-23010-5, 2021.

Etminan, M., Myhre, G., Highwood, E. J., and Shine, K. P.: Radiative forcing of carbon dioxide, methane, and nitrous oxide: A significant revision of the methane radiative forcing, Geophysical Research Letters, 43, https://doi.org/10.1002/2016GL071930, 2016.

Friedlingstein, P., O' Sullivan, M., Jones, M. W., Andrew, R. M., Hauck, J., Olsen, A., Peters, G. P., Peters, W., Pongratz, J., Sitch, S., Le Quéré, C., Canadell, J. G., Ciais, P., Jackson, R. B., Alin,

S., Aragão, L. E. O. C., Arneth, A., Arora, V., Bates, N. R., Becker, M., Benoit-Cattin, A., Bittig, H. C., Bopp, L., Bultan, S., Chandra, N., Chevallier, F., Chini, L. P., Evans, W., Florentie, L., Forster, P. M., Gasser, T., Gehlen, M., Gilfillan, D., Gkritzalis, T., Gregor, L., Gruber, N., Harris, I., Hartung, K., Haverd, V., Houghton, R. A., Ilyina, T., Jain, A. K., Joetzjer, E., Kadono, K., Kato, E., Kitidis, V., Korsbakken, J. I., Landschützer, P., Lefèvre, N., Lenton, A., Lienert, S., Liu, Z., Lombardozzi, D., Marland, G., Metzl, N., Munro, D. R., Nabel, J. E. M. S., Nakaoka, S.-I., Niwa, Y., O' Brien, K., Ono, T., Palmer, P. I., Pierrot, D., Poulter, B., Resplandy, L., Robertson, E., Rödenbeck, C., Schwinger, J., Séférian, R., Skjelvan, I., Smith, A. J. P., Sutton, A. J., Tanhua, T., Tans, P. P., Tian, H., Tilbrook, B., van der Werf, G., Vuichard, N., Walker, A. P., Wanninkhof, R., Watson, A. J., Willis, D., Wiltshire, A. J., Yuan, W., Yue, X., and Zaehle, S.: Global Carbon Budget 2020, Earth System Science Data, 12, 3269 – 3340, https://doi.org/10.5194/essd-12-3269-2020, 2020.

Gasser, T., Kechiar, M., Ciais, P., Burke, E. J., Kleinen, T., Zhu, D., Huang, Y., Ekici, A., and Obersteiner, M.: Path-dependent reductions in CO2 emission budgets caused by permafrost carbon release, Nature Geoscience, 11, 830 – 835, https://doi.org/10.1038/s41561-018-0227-0, 2018.

Gulev, S. K., Thorne, P. W., Ahn, J., Dentener, F. J., Domingues, C. M., Gerland, S., Gong, D., Kaufman, D. S., Nnamchi, H. C., Quaas, J., Rivera, J. A., Sathyendranath, S., Smith, S. L., Trewin, B., von Schuckmann, K., Vose, R. S., Allan, R., Collins, B., Turner, A., and Hawkins, E.: Changing state of the climate system, edited by: Masson-Delmotte, V., Zhai, P., Pirani, A., Connors, S. L., Pé an, C., Berger, S., Caud, N., Chen, Y., Goldfarb, L., Gomis, M. I., Huang, M., Leitzell, K., Lonnoy, E., Matthews, J. B. R., Maycock, T. K., Waterfield, T., Yelekçi, O., Yu, R., and Zhou, B., Cambridge University Press, Cambridge, UK, 287 – 422, 2021.

Hugelius, G., Strauss, J., Zubrzycki, S., Harden, J. W., Schuur, E. a. G., Ping, C.-L., Schirrmeister, L., Grosse, G., Michaelson, G. J., Koven, C. D., O'Donnell, J. A., Elberling, B., Mishra, U., Camill, P., Yu, Z., Palmtag, J., and Kuhry, P.: Estimated stocks of circumpolar permafrost carbon with quantified uncertainty ranges and identified data gaps, Biogeosciences, 11, 6573–6593, https://doi.org/10.5194/bg-11-6573-2014, 2014.

Kleinen, T. and Brovkin, V.: Pathway-dependent fate of permafrost region carbon, Environmental Research Letters, 13, 094001, https://doi.org/10.1088/1748-9326/aad824, 2018.

Koven, C., Friedlingstein, P., Ciais, P., Khvorostyanov, D., Krinner, G., and Tarnocai, C.: On the formation of high-latitude soil carbon stocks: Effects of cryoturbation and insulation by organic matter in a land surface model, Geophysical Research Letters, 36, https://doi.org/10.1029/2009GL040150, 2009.

MacDougall, A. H.: Reversing climate warming by artificial atmospheric carbon-dioxide removal: Can a Holocene-like climate be restored? Geophysical Research Letters, 40, 5480 - 5485, https://doi.org/10.1002/2013GL057467, 2013.

MacDougall, A. H., Zickfeld, K., Knutti, R., and Matthews, H. D.: Sensitivity of carbon budgets to permafrost carbon feedbacks and non-CO2 forcings, Environmental Research Letters, 10, 125003, https://doi.org/10.1088/1748-9326/10/12/125003, 2015.

MacDougall, A. H. and Knutti, R.: Projecting the release of carbon from permafrost soils using a perturbed parameter ensemble modelling approach, Biogeosciences, 13, 2123–2136, https://doi.org/10.5194/bg-13-2123-2016, 2016.

MacDougall, A. H.: Estimated effect of the permafrost carbon feedback on the zero emissions commitment to climate change, Biogeosciences, 18, 4937–4952, https://doi.org/10.5194/bg-18-4937-2021, 2021.

McKay, M. D., Beckman, R. J., and Conover, W. J.: A Comparison of Three Methods for Selecting Values of Input Variables in the Analysis of Output from a Computer Code, Technometrics, 21, 239 - 245, https://doi.org/10.2307/1268522, 1979.

Meissner, K. J., Weaver, A. J., Matthews, H. D., and Cox, P. M.: The role of land surface dynamics in glacial inception: a study with the UVic Earth System Model, Climate Dynamics, 21, 515–537, https://doi.org/10.1007/s00382-003-0352-2, 2003.

Mengis, N., Keller, D. P., MacDougall, A. H., Eby, M., Wright, N., Meissner, K. J., Oschlies, A., Schmittner, A., MacIsaac, A. J., Matthews, H. D., and Zickfeld, K.: Evaluation of the University of Victoria Earth System Climate Model version 2.10 (UVic ESCM 2.10), Geoscientific Model Development, 13, 4183–4204, https://doi.org/10.5194/gmd-13-4183-2020, 2020.

Natali, S. M., Holdren, J. P., Rogers, B. M., Treharne, R., Duffy, P. B., Pomerance, R., and MacDonald, E.: Permafrost carbon feedbacks threaten global climate goals, Proceedings of the National Academy of Sciences, 118, e2100163118, https://doi.org/10.1073/pnas.2100163118, 2021.

Pearson, R. G., Phillips, S. J., Loranty, M. M., Beck, P. S. A., Damoulas, T., Knight, S. J., and Goetz, S. J.: Shifts in Arctic vegetation and associated feedbacks under climate change, Nature Climate Change, 3, 673 – 677, https://doi.org/10.1038/nclimate1858, 2013.

Schuur, E. a. G., McGuire, A. D., Schädel, C., Grosse, G., Harden, J. W., Hayes, D. J., Hugelius, G., Koven, C. D., Kuhry, P., Lawrence, D. M., Natali, S. M., Olefeldt, D., Romanovsky, V. E., Schaefer, K., Turetsky, M. R., Treat, C. C., and Vonk, J. E.: Climate change and the permafrost carbon feedback, Nature, 520, 171 - 179, https://doi.org/10.1038/nature14338, 2015.

Schwinger, J., Asaadi, A., Steinert, N. J., and Lee, H.: Emit now, mitigate later? Earth system reversibility under overshoots of different magnitudes and durations, Earth System Dynamics, 13, 1641 – 1665, https://doi.org/10.5194/esd-13-1641-2022, 2022.

Strauss, J., Schirrmeister, L., Grosse, G., Fortier, D., Hugelius, G., Knoblauch, C., Romanovsky, V., Schädel, C., Schneider von Deimling, T., Schuur, E. A. G., Shmelev, D., Ulrich, M., and Veremeeva, A.: Deep Yedoma permafrost: A synthesis of depositional characteristics and carbon vulnerability, Earth-Science Reviews, 172, 75 – 86, https://doi.org/10.1016/j.earscirev.2017.07.007, 2017.

Strauss, J., Laboor, S., Schirrmeister, L., Fedorov, A. N., Fortier, D., Froese, D., Fuchs, M., Günther, F., Grigoriev, M., Harden, J., Hugelius, G., Jongejans, L. L., Kanevskiy, M., Kholodov, A., Kunitsky,

V., Kraev, G., Lozhkin, A., Rivkina, E., Shur, Y., Siegert, C., Spektor, V., Streletskaya, I., Ulrich, M., Vartanyan, S., Veremeeva, A., Anthony, K. W., Wetterich, S., Zimov, N., and Grosse, G.: Circum-Arctic Map of the Yedoma Permafrost Domain, Frontiers in Earth Science, 9, 758360, https://doi.org/10.3389/feart.2021.758360, 2021.

Strauss, J., Laboor, S., Schirrmeister, L., Fedorov, A. N., Fortier, D., Froese, D. G., Fuchs, M., Günther, F., Grigoriev, M. N., Harden, J. W., Hugelius, G., Jongejans, L. L., Kanevskiy, M. Z., Kholodov, A. L., Kunitsky, V., Kraev, G., Lozhkin, A. V., Rivkina, E., Shur, Y., Siegert, C., Spektor, V., Streletskaya, I., Ulrich, M., Vartanyan, S. L., Veremeeva, A., Walter Anthony, K. M., Wetterich, S., Zimov, N. S., and Grosse, G.: Database of Ice-Rich Yedoma Permafrost Version 2 (IRYP v2), PANGAEA, https://doi.org/10.1594/PANGAEA.940078, 2022.

Tokarska, K. B. and Zickfeld, K.: The effectiveness of net negative carbon dioxide emissions in reversing anthropogenic climate change, Environmental Research Letters, 10, 094013, https://doi.org/10.1088/1748-9326/10/9/094013, 2015.

Zhang, T., Heginbottom ,J. A., Barry ,R. G., and Brown, J.: Further statistics on the distribution of permafrost and ground ice in the Northern Hemisphere 1, Polar Geography, 24, 126 – 131, https://doi.org/10.1080/10889370009377692, 2000.

Zimov, S. A., Schuur, E. A. G., and Chapin, F. S.: Permafrost and the Global Carbon Budget, Science, 312, 1612 – 1613, https://doi.org/10.1126/science.1128908, 2006.

# Referee #2

## Overall:

This study "aims to fill these gaps using an Earth system model of intermediate complexity to systematically assess the permafrost response and feedback under temperature stabilization or overshoot scenarios achieving various GWLs." I think it is an interesting paper and recommend publication, but I also think it could make some clearer points, as I discuss below.

Based on that stated aim, I expected to see one or more figures with total permafrost carbon losses plotted as a function of the GWL for both the stabilization and overshoot cases. I.e., is the permafrost carbon loss linear? Are there thresholds or tipping points? Figure 6a shows the areal loss as a function of global warming level, but why are carbon variables not quantified in this way? Does the permafrost carbon feedback strength (in units of Pg C / degree Celsius warming) show a similar nonlinearity as the SPAW shown in f.g 6a with maximum losses per unit warming in the 1.5-2 degree C range? Figure 3b seems to show that the highest sensitivity is in the ~3 degree warming range, but it is difficult to see quantitatively. Likewise it would be interesting to se the radiative forcing as well. So I'd recommend an additional figure with panels along the lines of 6a that allows the reader to trace how the (non-)linearity of each of these permafrost metrics as a function of global warming levels for the stabilization and overshoot cases changes between permafrost area, permafrost carbon, and permafrost radiative forcing.

Thank you for your insightful suggestion. We fully agree that using global warming levels (GWLs) as the horizontal axis to present key permafrost metrics helps reveal their linear or nonlinear behavior. In response, we have added a new Section, "3.3 Linearity of Permafrost Response and Feedback", along with a new figure (Figure 10) to the revised manuscript. This figure includes three panels showing (a) permafrost area loss, (b) permafrost carbon loss, and (c) permafrost radiative forcing, all plotted as a function of GWLs. To further explore the potential for thresholds or tipping points, we have also added Figure 8 and corresponding text to examine the evolution of the permafrost feedback factor across scenarios.

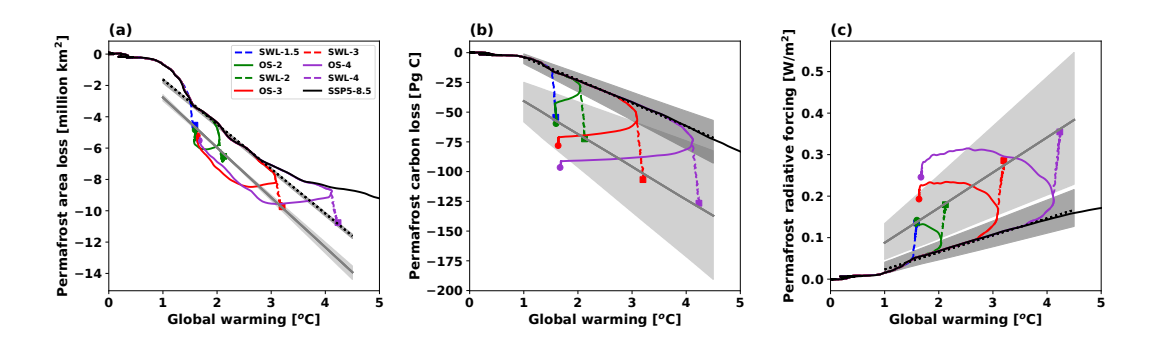


Figure 10. Relationship between global warming levels and three permafrost metrics: (a) permafrost area loss, (b) permafrost carbon loss, and (c) permafrost radiative forcing in the stabilization (colored dashed lines) and overshoot (colored solid lines) scenarios at 1.5 °C (blue), 2.0 °C (green), 3.0 °C (red) and 4.0 °C (purple) global warming levels, along with the SSP5-8.5 scenario (black).

Square and circle markers indicate values in the year 2300 for the stabilization and overshoot scenarios, respectively. All results are based on the PFC simulations. Grey solid lines show linear fits of permafrost metrics to global warming levels in stabilization scenarios by 2300, while black dashed lines show corresponding fits for the SSP5-8.5 scenario. Note that in panel (a), both the stabilization scenarios and the corresponding SSP5-8.5 points included in the linear fit are limited to global warming levels between 1.5 °C and 3.0 °C, whereas in panels (b) and (c), the fits include points with global warming levels ranging from 1.5 °C to 4.0 °C. For stabilization scenarios, only the results from the year 2300 are used for fitting, while for the SSP5-8.5 scenario, all results within the specified global warming level ranges are used for fitting. Shaded regions represent the 5th to 95th percentile ranges across 250 ensemble simulations.

The new Section "3.3 Linearity of Permafrost Response and Feedback" is as following:

"After exploring the response and feedback of permafrost under temperature stabilization and overshoot scenarios at various global warming levels, it is natural to question the (non-)linearity of these response and feedback as functions of global warming levels. Our results show that the responses of permafrost area, permafrost carbon feedback and associated radiative forcing to a broad range of global warming are nearly linear (Fig. 10). The permafrost area change exhibits a strongly nonlinear relationship with global warming below 1.5 °C level, then a quasilinear relation between them in the global warming ranges from 1.5 °C to 3 °C. Above 3 °C global warming, the sensitivity of permafrost area to global warming decreases nonlinearly, and it is evident in both stabilization and SSP5-8.5 scenarios (Fig. 10a). In contrast, permafrost carbon loss and associated radiative forcing exhibit a nearly linear response to increasing global warming levels, especially above 1 °C, for both stabilization and SSP5-8.5 scenarios (Fig. 10b, c)."

"Meanwhile, the sensitivities of permafrost area, permafrost carbon loss, and associated radiative forcing to global warming under stabilization scenarios are all stronger than those under the SSP5-8.5 scenario. Specifically, based on the simulated permafrost area in the year 2300 under stabilization scenarios with global warming levels between 1.5 °C and 3 °C, the sensitivity of permafrost area to global warming is -3.19 [-3.01 to -3.36] million km<sup>2</sup> °C<sup>-1</sup>. In comparison, a linear fit of permafrost area change against global warming levels over the same temperature range in the SSP5-8.5 scenario yields a sensitivity of -2.85 [-2.77 to -2.89] million km<sup>2</sup> °C<sup>-1</sup>. Similarly, the permafrost carbon feedback per degree of global warming derived from a linear fit based on the total permafrost carbon loss in the year 2300 under stabilization scenarios, is -27.6 [-16.5 to -38.2] PgC °C<sup>-1</sup>. In contrast, the corresponding value under the SSP5-8.5 scenario, estimated from a linear fit over the 1.5 °C to 4.0 °C warming range, is -19.3 [-15.7 to -24.1] PgC °C<sup>-1</sup>. Applying the same approach, the associated radiative forcing per degree of global warming is estimated to be 0.08 [0.05 to 0.12] W m<sup>-2</sup> °C<sup>-1</sup> for the stabilization scenarios and 0.04 [0.03 to 0.05] W m<sup>-2</sup> °C<sup>-1</sup> for the SSP5-8.5. These differences between the stabilization and SSP5-8.5 scenarios are mainly attributable to the differing response time scales represented by the two scenarios: SSP5-8.5 reflects a typical transient response, while the stabilization scenarios maintain stabilized temperatures over extended periods and thus approximate a quasi-equilibrium response of the climate-carbon system. Furthermore, the smaller sensitivity of permafrost radiative forcing per degree of global warming under the SSP5-8.5 can be partially attributed to its higher background atmospheric CO2 concentration compared to the stabilization scenarios. The same amount of CO2 emissions would produce smaller additional radiative forcing under a higher background atmospheric CO<sub>2</sub> concentration, due to the logarithmic relationship between CO<sub>2</sub> concentration and radiative forcing (Etminan et al., 2016)."

"To a certain extent, our findings align with those of Nitzbon et al. (2024), who suggested that the accumulated response of Arctic permafrost to climate warming is approximately quasilinear. Nitzbon et al. (2024) reported a quasilinear decrease in the equilibrium permafrost extent to global warming, with a rate of approximately 3.5 million km² °C¹. This quasilinear relation holds for global warming ranges from 0 °C to 4 °C, derived from the empirical relationship between the local permafrost fraction and the annual mean global temperature. However, our results indicate the quasilinear relationship only holds for global warming levels between 1.5 °C and 3 °C. Furthermore, the permafrost carbon feedback and the associated radiative forcing per degree of warming, as derived from our simulations of both stabilization and SSP5-8.5 scenarios, are within the ranges of -18 [-3.1 to -41] PgC °C¹ and 0.09 [0.02 to 0.20] W m² °C¹, respectively, reported by Canadell et al. (2021). Our estimates also align with the estimated range of equilibrium sensitivity of permafrost carbon decline to global warming, which is -21 [-4 to -48] PgC °C¹. This may represent an upper limit for permafrost carbon feedback per degree of global warming, considering that the estimated reduction in permafrost carbon does not equate directly to carbon emissions released into the atmosphere, as noted by Nitzbon et al. (2024)."

"Under overshoot scenarios, permafrost area responds nearly reversibly and presents an almost closed loop (Fig. 10a). In contrast, permafrost carbon loss exhibits an open loop with respect to global warming levels. In other words, permafrost carbon loss does not reverse as temperatures decline, indicating irreversible permafrost carbon radiative forcing. Among the three metrics investigated here, only permafrost area exhibits strong reversibility under the overshoot scenarios. This also explains why, in Fig. 9a, the permafrost area sensitivity derived from the SSP5-8.5 scenario, when multiplied by additional warming, can reasonably reconstruct permafrost area loss in the stabilization and overshoot cases."

Figure 8 and corresponding text has been added to Section "3.2 Radiative Impacts of Permafrost Carbon Release" as follows:

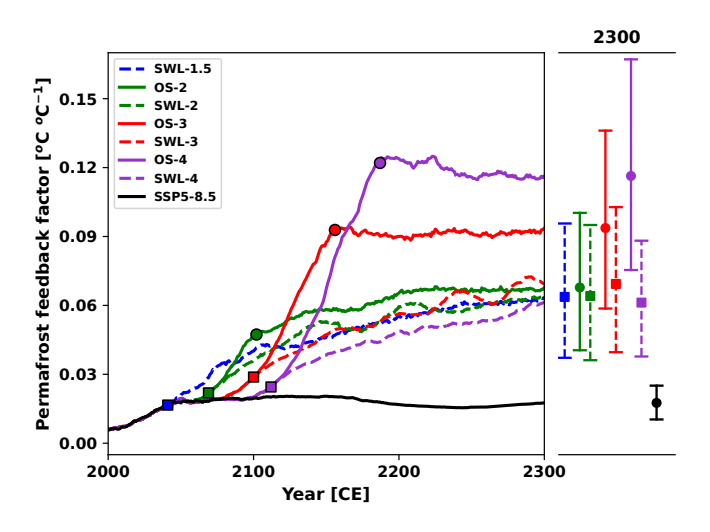


Figure 8. Timeseries of permafrost feedback factor under stabilization (dashed lines) and overshoot (solid lines) scenarios at 1.5 °C (blue), 2.0 °C (green), 3.0 °C (red), and 4.0 °C (purple) global warming levels, as well as the SSP5-8.5 scenario. Square markers indicate the time points when the temperature overshoot reaches its peak or stabilized warming begins, while circle markers indicate when the overshoot returns to 1.5 °C. Results represent the ensemble median of 250 simulations. Dots on the right panels represent values in the year 2300, with uncertainty ranges estimated as the 5th to 95th percentiles. The permafrost feedback factor is calculated as the ratio of additional global warming caused by the permafrost carbon feedback (i.e., the difference between the PFC and NPFC simulations) to the global mean temperature change in the NPFC simulations.

"The additional warming caused by permafrost carbon release can be utilized to assess whether the permafrost carbon feedback could be classified as a global tipping point process. This means it is not only positive but also sufficiently strong to sustain itself. To qualify, an initial rise in global mean temperature would need to trigger permafrost carbon emissions that result in a further increase in global mean temperature surpassing the initial warming. As a result, the positive permafrost carbon feedback would induce sufficient additional thawing to initiate a self-sustaining feedback loop (Nitzbon et al., 2024). We employed the permafrost feedback factor, which is defined as the ratio of the additional warming to the initial warming simulated with the permafrost carbon module deactivated, to determine if the permafrost carbon feedback can be considered as a global tipping process. In all perturbed parameter ensemble simulations for the stabilization, overshoot and SSP5-8.5 scenarios, the maximum permafrost feedback factor is 0.21 °C °C-1. By 2300, the permafrost feedback factor for the OS4 and SSP5-8.5 scenarios are estimated at 0.12 [0.08 to 0.17] °C °C<sup>-1</sup> and 0.02 [0.01-0.03] °C °C<sup>-1</sup>, respectively. The permafrost feedback parameter is the highest under the OS4 scenario, while it is the lowest under the SSP5-8.5 scenario (Fig. 8; Fig. S5). Interestingly, the feedback factors are quite similar across the stabilization scenarios, with values of 0.064 [0.037 to 0.096] °C °C<sup>-1</sup>, 0.064 [0.036 to 0.095] °C °C<sup>-1</sup>, 0.069 [0.040 to 0.103] °C °C<sup>-1</sup> and 0.061 [0.038 to 0.089] °C °C<sup>-1</sup> for the SWL-1.5, SWL-2, SWL-3 and SWL-4 scenarios by 2300, respectively. Although the feedback factor in the overshoot scenarios is substantially larger than the recent estimate of 0.035 (0.004-0.110) °C °C-1 based on the Sixth Assessment Report of the Intergovernmental Panel on Climate Change (Nitzbon et al., 2024), our findings indicate that the positive permafrost carbon feedback is unlikely to result in enough additional thawing and corresponding carbon emissions to initiate a self-perpetuating tipping process. Since this study only models the gradual thawing of permafrost through the deepening of the active layer, we cannot rule out the possibility of tipping points associated with the abrupt thawing of talik development, thermokarst and thermo-erosion processes."

Further, given the possibility of perturbing parameters due to the relatively low cost of running UVic-ESCM, I had expected to see if any of those parameters introduced nonlinearities or substantially changed the magnitude of the results. But I just see median lines. So it is hard to know how important the uncertainty is. I suggest showing the uncertainty via translucent colored plumes in all figures.

We sincerely appreciate your valuable suggestion. We fully acknowledge the importance of showing the uncertainty to accurately convey the results. In the revised manuscript, we have explicitly represented the 5th to 95th percentile of 250 ensemble simulations for the year 2300 in all relevant

figures to help readers better understand the uncertainty associated with parameter perturbations. For example, Figures 3, 5 and 7 now include uncertainty ranges using vertical bars. In addition, we have provided translucent colored plumes in the Supplementary Information (Figure S1–S5) to illustrate the full time-evolving uncertainty across all ensemble members.

The updated figures with uncertainty ranges are shown below:

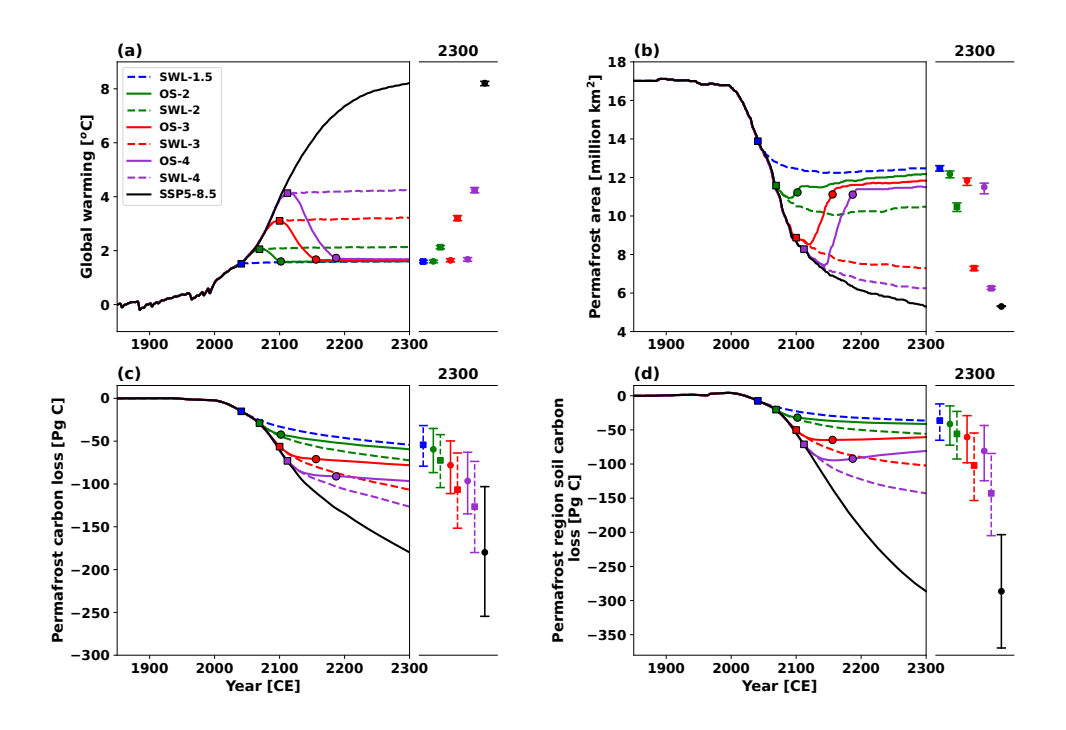


Figure 3. Timeseries of annual mean (a) global warming, (b) permafrost area, (c) permafrost carbon loss and (d) permafrost region soil carbon loss under stabilization (dashed lines) and overshoot (solid lines) scenarios at 1.5 °C (blue), 2.0 °C (green), 3.0 °C (red), and 4.0 °C (purple) global warming levels, as well as the SSP5-8.5 scenario. Square markers indicate the time points when the temperature overshoot reaches its peak or stabilized warming begins, while circle markers indicate when the overshoot returns to 1.5 °C. All changes are relative to the pre-industrial period (1850-1900). Results represent the ensemble median of 250 simulations based on the PFC simulations. Dots on the right panels represent values in the year 2300, with uncertainty ranges estimated as the 5th to 95th percentiles.

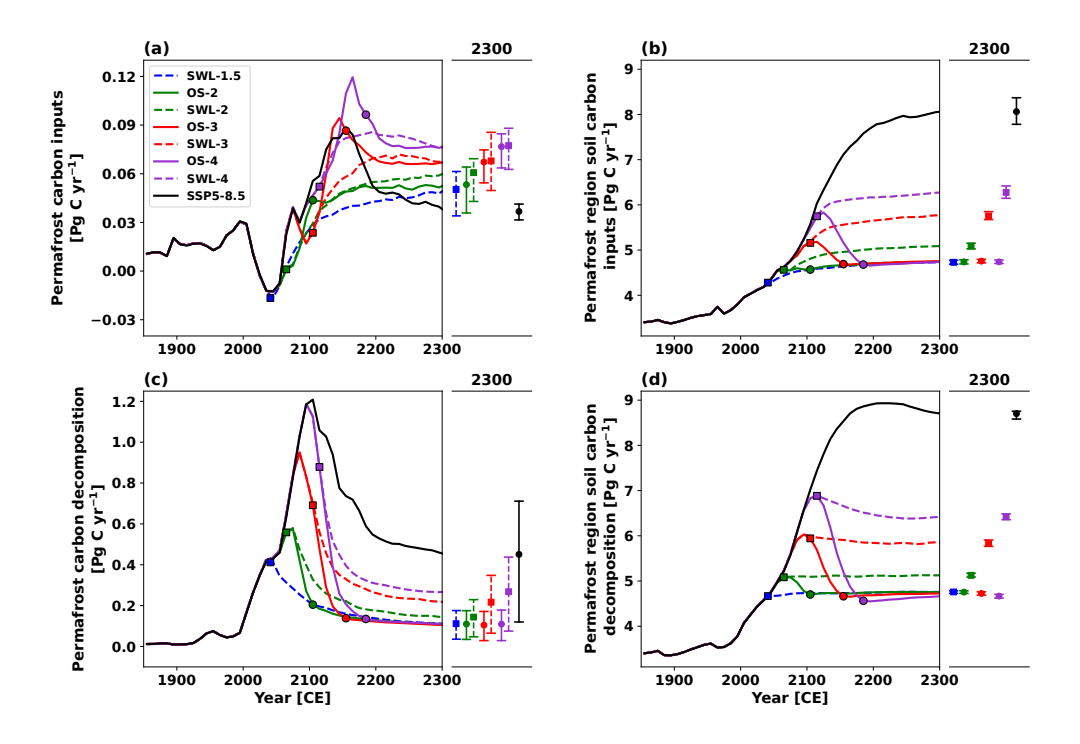


Figure 5. Timeseries of changes in (a) permafrost carbon inputs, (b) permafrost region soil carbon inputs, (c) permafrost carbon decomposition and (d) permafrost region soil carbon decomposition, under the stabilization (dashed lines) and overshoot (solid lines) scenarios at 1.5 °C (blue), 2.0 °C (green), 3.0 °C (red) and 4.0 °C (purple) GWLs, along with the SSP5-8.5 scenario (black). Square markers indicate the time points when the temperature overshoot reaches its peak or stabilized warming begins, while circle markers indicate when the overshoot returns to 1.5 °C. Results represent the ensemble median of 250 simulations based on the PFC simulations. Dots on the right panels represent values in the year 2300, with uncertainty ranges estimated as the 5th to 95th percentiles.

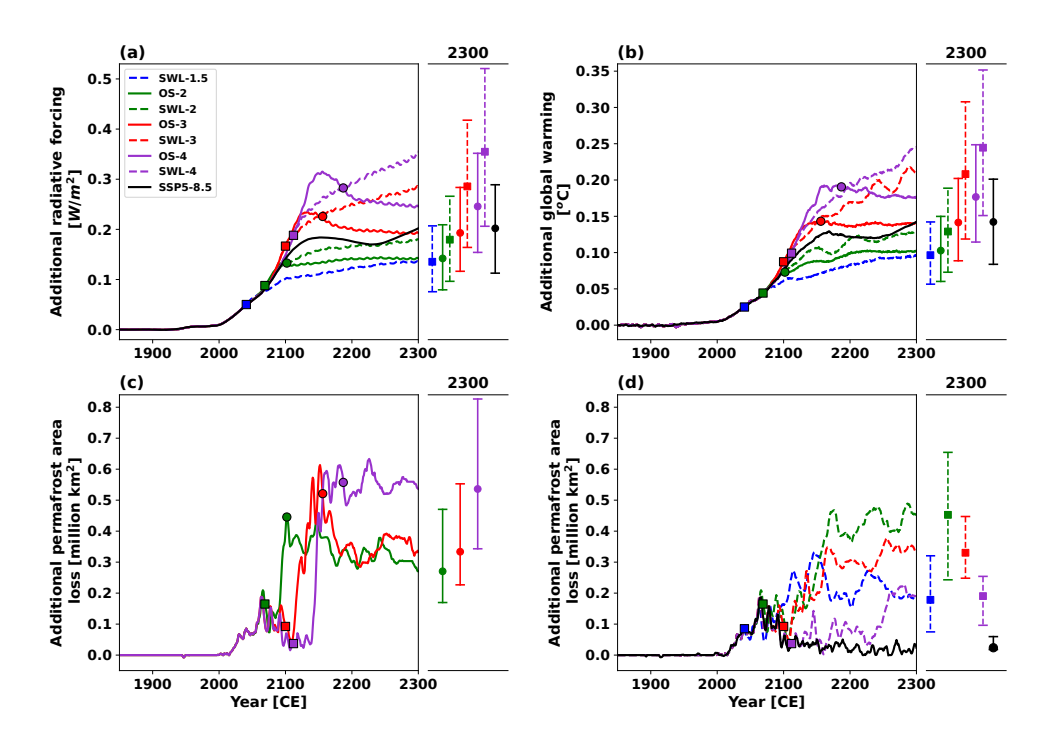


Figure 7. Additional changes in (a) radiative forcing, (b) global warming and (c, d) permafrost area due to permafrost carbon feedback, calculated as the difference between the PFC and NPFC simulations. Shown are results for the stabilization (dashed lines) and overshoot (solid lines) scenarios at 1.5 °C (blue), 2.0 °C (green), 3.0 °C (red) and 4.0 °C (purple) global warming levels, along with the SSP5-8.5 scenario (black). Square markers indicate the time points when the temperature overshoot reaches its peak or stabilized warming begins, while circle markers indicate when the overshoot returns to 1.5 °C. Results represent the ensemble median of 250 simulations. Dots on the right panels represent values in the year 2300, with uncertainty ranges estimated as the 5th to 95th percentiles. In panel (a), the additional radiative forcing is calculated using the simplified expressions (Etminan et al., 2016) based on simulated CO<sub>2</sub> concentrations. In panels (c) and (d), the additional permafrost area loss is smoothed using a 5-year rolling average to eliminate interannual variability.

#### Comments

line 36: the 1.5 degree budget will be exhausted within the next few years, but not the 2 degree budget. Please clarify.

Thank you for your suggestion. We have revised the sentence for greater clarity:

"If current emission rates persist, the remaining carbon budgets compatible with the 1.5 °C target will be critically tight and likely exhausted within the next few years (Rogelj et al., 2015; Goodwin et al., 2018; Masson-Delmotte et al., 2018; Forster et al., 2023; Smith et al., 2023)."

Paragraph starting line 142: This is great that you were able to perturb these key parameters. But I don't see any uncertainty plumes in any of the figures, only the median values. I think it would be informative to the reader to see the parameter uncertainty plumes plotted on all figures.

Thank you for your comment. As noted above, we have incorporated the 5th to 95th percentiles of 250 ensemble simulations for the year 2300 in all relevant figures. Additionally, time-evolving uncertainty associated with the perturbed parameters is illustrated using translucent colored plumes in the Supplementary Information (Figs. S1–S5).

fig. 2b: Why doesn't the permafrost area recover all the way under the overshoot scenarios? Are there regional changes to the northern high latitude climate that are responsible for the differing permafrost amounts at a given GWL? If so, what are the drivers of that regional change? It might help to add a panel with the regional temperature difference to see whether it behaves differently from the global mean.

Thank you for your valuable comments. In response, we plotted a new figure (Figure R2) to quantify additional warming in permafrost regions and to examine the regional amplification relative to the global mean. We added the following paragraph in Section "4 Conclusion and Discussion" to explain why the permafrost area does not recover all the way under the overshoot scenarios:

"Our results show incomplete recovery of permafrost area under the overshoot scenarios, which is influenced by multiple factors: First, the additional permafrost carbon release leads to greater additional warming under the overshoot scenarios than the SWL-1.5 scenario, causing additional permafrost degradation. By 2300, the northern high-latitude permafrost regions are 0.01~0.13 °C warmer compared to the SWL-1.5 scenario. Second, the thermal inertia of deep soil layers limits the rate of permafrost recovery. Even after global mean temperatures return to the 1.5 °C target, residual heat accumulated in deeper soil layers during temperature overshoot period continues to inhibit permafrost refreezing, preventing full restoration to its pre-overshoot state. Third, greater soil carbon loss under overshoot scenarios substantially alters the hydrological and thermal properties of soil, affecting the processes that govern carbon cycling (Zhu et al., 2019; Avis, 2012; Lawrence and Slate, 2008), which in turn affects the recovery of permafrost area. Moreover, irreversible shifts in vegetation composition of high-latitude terrestrial ecosystems also contribute to the incomplete recovery of permafrost area under overshoot scenarios. For instance, among the two dominant vegetation types, needleleaf trees continue to expand while C3 grasses decline, even after global temperatures return to the 1.5 °C warming level. These irreversible changes may stabilize the carbon, water, and energy cycles over the permafrost region at different equilibria after overshoot, through the interactions between physical and biophysical processes (de Vrese and Brovkin, 2021), thereby constraining the ability of permafrost to fully recover under the overshoot scenarios."

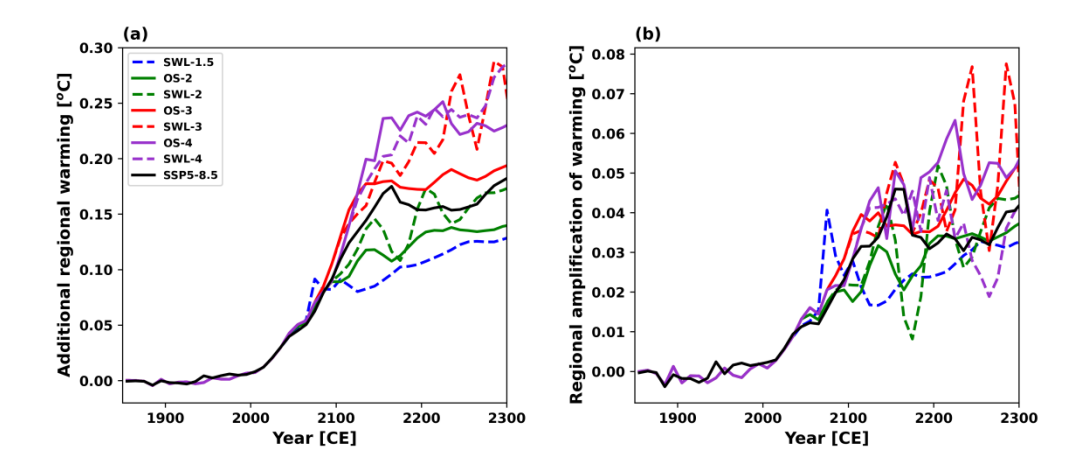


Figure R2. Timeseries of changes relative to the SWL-1.5 scenario for the overshoot scenarios at 2.0 °C (green), 3.0 °C (red), and 4.0 °C (purple) global warming levels. Panel (a) shows the additional warming in permafrost regions, calculated as the difference between the PFC and NPFC simulations. Panel (b) shows the regional amplification of warming, defined as the difference between additional warming in permafrost regions and the corresponding additional global warming.

Line 321: This paper doesn't really establish anything about the realism of the model, since there are no model-data comparisons, so suggest reword or provide citations to the papers that have shown this.

Thank you for your valuable comment. We acknowledge the need for additional clarification regarding the realism of the UVic ESCM model. To address this, we have incorporated model validation into the first paragraph of Section "3 Results". This addition provides a direct comparison

between model simulations and observational data, demonstrating that the UVic ESCM model realistically reproduces historical permafrost area and permafrost carbon stocks. The added paragraph reads:

"The UVic ESCM v2.10 reliably simulates historical temperature changes, permafrost area, and the partitioning of anthropogenic carbon emissions among the atmosphere, ocean and land. Under preindustrial conditions, the simulated Northern Hemisphere permafrost area, defined as regions where the soil layer remains perennially frozen for at least two consecutive years, was 17.01 [17.00 to 17.04] million km<sup>2</sup>, the simulated total soil carbon stock in the permafrost regions was 1031 [915 to 1149] PgC, of which 484 [383 to 590] PgC was classified as perennially frozen carbon and 547 [533 to 559] PgC was classified as usual soil carbon. For the period 1960–1990, the model simulated Northern Hemisphere permafrost area at 16.8 [16.7 to 16.9] million km<sup>2</sup>, which falls within the reconstructed range from 12.0 to 18.2 million km<sup>2</sup> (Chadburn et al., 2017) and the observation derived extent from 12.21 to 16.98 million km<sup>2</sup> (Zhang et al., 2000). Additionally, the simulated soil carbon stock in the top 3.35 m of permafrost regions for this same period was 1034 [919 to 1151] PgC, with 483 [382 to 587] PgC classified as perennially frozen carbon, accounting for 47% [42% to 51%] of the total permafrost soil carbon stock, in agreement with Hugelius et al. (2014). During the period 2011-2020, the model estimated a global mean temperature increase of 1.14 [1.13 to 1.15] °C relative to preindustrial levels, which is closely aligned with the observed rise of 1.09 [0.91 to 1.23] °C (Gulev et al., 2021). From 2010 to 2019, the model estimated that anthropogenic carbon emissions were distributed as follows: 5.5 [5.4 to 5.6] PgC yr<sup>-1</sup> to the atmosphere, 3.0 [2.98 to 3.03] PgC yr<sup>-1</sup> to the ocean, and 2.5 [2.4 to 2.6] PgC yr<sup>-1</sup> to terrestrial ecosystems. These estimates are broadly consistent with the global anthropogenic CO<sub>2</sub> budget assessment by the Global Carbon Project (GCP) with figures of 5.1±0.02 PgC yr<sup>-1</sup> for the atmosphere, 2.5±0.6 PgC yr<sup>-1</sup> for the ocean, and 3.4±0.9 PgC yr<sup>-1</sup> for terrestrial ecosystems (Friedlingstein et al., 2020)."

Accordingly, we have revised the statement in Line 321 to: "The UVic ESCM has been validated against observational and reconstructed datasets, demonstrating its ability to reproduce historical permafrost area and permafrost carbon stocks."

Data availability: I downloaded some of the data files in Cui et al., 2024, but they aren't clearly described and don't include any further details than what is in the paper (e.g., spatial information). This strikes me as a fairly minimal data archival effort.

We appreciate your comments regarding the data archiving. We have added more detailed descriptions to the uploaded data files, including variable names, units, and associated spatial and temporal dimensions, in order to improve the clarity.

Due to the large volume of spatial model output, we have archived only the key variables necessary to support the main analyses presented in the paper (https://zenodo.org/records/15148252). Although this may not capture all details, we are happy to provide more comprehensive datasets upon request. In addition, a data description file (README.md) has been included alongside the archived model output to facilitate understanding.

## References

Avis, C. A., Weaver, A. J., and Meissner, K. J.: Reduction in areal extent of high-latitude wetlands in response to permafrost thaw, Nature Geoscience, 4, 444–448, https://doi.org/10.1038/ngeo1160, 2011.

Canadell, J., Forster, P., Meyer, C., and the Chapter 5 authors: Global carbon and other biogeochemical cycles and feedbacks, in: Climate Change 2021: The Physical Science Basis. Contribution of Working Group I to the Sixth Assessment Report of the Intergovernmental Panel on Climate Change, edited by: Masson-Delmotte, V., Zhai, P., Pirani, A., et al., Cambridge University Press, Cambridge, United Kingdom and New York, NY, USA, Chapter 5, https://doi.org/10.1017/9781009157896.007, 2021.

Chadburn, S. E., Burke, E. J., Cox, P. M., Friedlingstein, P., Hugelius, G., and Westermann, S.: An observation-based constraint on permafrost loss as a function of global warming, Nature Climate Change, 7, 340 – 344, https://doi.org/10.1038/nclimate3262, 2017.

De Vrese, P. and Brovkin, V.: Timescales of the permafrost carbon cycle and legacy effects of temperature overshoot scenarios, Nature Communications, 12, 2688, https://doi.org/10.1038/s41467-021-23010-5, 2021.

Etminan, M., Myhre, G., Highwood, E. J., and Shine, K. P.: Radiative forcing of carbon dioxide, methane, and nitrous oxide: A significant revision of the methane radiative forcing, Geophysical Research Letters, 43, https://doi.org/10.1002/2016GL071930, 2016.

Forster, P. M., Smith, C. J., Walsh, T., Lamb, W. F., Lamboll, R., Hauser, M., Ribes, A., Rosen, D., Gillett, N., Palmer, M. D., Rogelj, J., von Schuckmann, K., Seneviratne, S. I., Trewin, B., Zhang, X., Allen, M., Andrew, R., Birt, A., Borger, A., Boyer, T., Broersma, J. A., Cheng, L., Dentener, F., Friedlingstein, P., Gutiérrez, J. M., Gütschow, J., Hall, B., Ishii, M., Jenkins, S., Lan, X., Lee, J.-Y., Morice, C., Kadow, C., Kennedy, J., Killick, R., Minx, J. C., Naik, V., Peters, G. P., Pirani, A., Pongratz, J., Schleussner, C.-F., Szopa, S., Thorne, P., Rohde, R., Rojas Corradi, M., Schumacher, D., Vose, R., Zickfeld, K., Masson-Delmotte, V., and Zhai, P.: Indicators of Global Climate Change 2022: annual update of large-scale indicators of the state of the climate system and human influence, Earth System Science Data, 15, 2295 – 2327, https://doi.org/10.5194/essd-15-2295-2023, 2023.

Friedlingstein, P., O' Sullivan, M., Jones, M. W., Andrew, R. M., Hauck, J., Olsen, A., Peters, G. P., Peters, W., Pongratz, J., Sitch, S., Le Quéré, C., Canadell, J. G., Ciais, P., Jackson, R. B., Alin, S., Aragão, L. E. O. C., Arneth, A., Arora, V., Bates, N. R., Becker, M., Benoit-Cattin, A., Bittig, H. C., Bopp, L., Bultan, S., Chandra, N., Chevallier, F., Chini, L. P., Evans, W., Florentie, L., Forster, P. M., Gasser, T., Gehlen, M., Gilfillan, D., Gkritzalis, T., Gregor, L., Gruber, N., Harris, I., Hartung, K., Haverd, V., Houghton, R. A., Ilyina, T., Jain, A. K., Joetzjer, E., Kadono, K., Kato, E., Kitidis, V., Korsbakken, J. I., Landschützer, P., Lefèvre, N., Lenton, A., Lienert, S., Liu, Z., Lombardozzi, D., Marland, G., Metzl, N., Munro, D. R., Nabel, J. E. M. S., Nakaoka, S.-I., Niwa, Y., O' Brien, K., Ono, T., Palmer, P. I., Pierrot, D., Poulter, B., Resplandy, L., Robertson, E., Rödenbeck, C., Schwinger, J., Séférian, R., Skjelvan, I., Smith, A. J. P., Sutton, A. J., Tanhua, T., Tans, P. P., Tian, H., Tilbrook, B., van der Werf, G., Vuichard, N., Walker, A. P., Wanninkhof, R., Watson, A. J., Willis,

D., Wiltshire, A. J., Yuan, W., Yue, X., and Zaehle, S.: Global Carbon Budget 2020, Earth System Science Data, 12, 3269 - 3340, https://doi.org/10.5194/essd-12-3269-2020, 2020.

Goodwin, P., Katavouta, A., Roussenov, V. M., Foster, G. L., Rohling, E. J., and Williams, R. G.: Pathways to 1.5 ° C and 2 ° C warming based on observational and geological constraints, Nature Geoscience, 11, 102 – 107, https://doi.org/10.1038/s41561-017-0054-8, 2018.

Gulev, S. K., Thorne, P. W., Ahn, J., Dentener, F. J., Domingues, C. M., Gerland, S., Gong, D., Kaufman, D. S., Nnamchi, H. C., Quaas, J., Rivera, J. A., Sathyendranath, S., Smith, S. L., Trewin, B., von Schuckmann, K., Vose, R. S., Allan, R., Collins, B., Turner, A., and Hawkins, E.: Changing state of the climate system, edited by: Masson-Delmotte, V., Zhai, P., Pirani, A., Connors, S. L., Pé an, C., Berger, S., Caud, N., Chen, Y., Goldfarb, L., Gomis, M. I., Huang, M., Leitzell, K., Lonnoy, E., Matthews, J. B. R., Maycock, T. K., Waterfield, T., Yelekçi, O., Yu, R., and Zhou, B., Cambridge University Press, Cambridge, UK, 287 – 422, 2021.

Hugelius, G., Strauss, J., Zubrzycki, S., Harden, J. W., Schuur, E. a. G., Ping, C.-L., Schirrmeister, L., Grosse, G., Michaelson, G. J., Koven, C. D., O'Donnell, J. A., Elberling, B., Mishra, U., Camill, P., Yu, Z., Palmtag, J., and Kuhry, P.: Estimated stocks of circumpolar permafrost carbon with quantified uncertainty ranges and identified data gaps, Biogeosciences, 11, 6573–6593, https://doi.org/10.5194/bg-11-6573-2014, 2014.

Lawrence, D. M. and Slater, A. G.: Incorporating organic soil into a global climate model, Clim Dyn, 30, 145 - 160, https://doi.org/10.1007/s00382-007-0278-1, 2008.

Masson-Delmotte, V., Zhai, P., Pörtner, H.-O., Roberts, D. C., Skea, J., Shukla, P. R., Pirani, A., Moufouma-Okia, W., Péan, C., Pidcock, R., Connors, S., Matthews, J. B. R., Yang, C., Zhou, X., and Steg, L.: Global warming of 1.5 ° C: Summary for policy makers, IPCC - The Intergovernmental Panel on Climate Change, https://doi.org/10.1017/9781009157940.001, 2018.

Nitzbon, J., Schneider Von Deimling, T., Aliyeva, M., Chadburn, S. E., Grosse, G., Laboor, S., Lee, H., Lohmann, G., Steinert, N. J., Stuenzi, S. M., Werner, M., Westermann, S., and Langer, M.: No respite from permafrost-thaw impacts in the absence of a global tipping point, Nature Climate Change, 14, 573 – 585, https://doi.org/10.1038/s41558-024-02011-4, 2024.

Rogelj, J., Meinshausen, M., Schaeffer, M., Knutti, R., and Riahi, K.: Impact of short-lived non-CO2 mitigation on carbon budgets for stabilizing global warming, Environmental Research Letters, 10, 075001, https://doi.org/10.1088/1748-9326/10/7/075001, 2015.

Smith, S., Geden, O., Nemet, G., Gidden, M., Lamb, W., Powis, C., Bellamy, R., Callaghan, M., Cowie, A., Cox, E., Fuss, S., Gasser, T., Grassi, G., Greene, J., Lueck, S., Mohan, A., Müller-Hansen, F., Peters, G., Pratama, Y., Repke, T., Riahi, K., Schenuit, F., Steinhauser, J., Strefler, J., Valenzuela, J., and Minx, J.: State of Carbon Dioxide Removal - 1st Edition, https://doi.org/10.17605/OSF.IO/W3B4Z, 2023.

Zhang, T., Heginbottom ,J. A., Barry ,R. G., and Brown, J.: Further statistics on the distribution of permafrost and ground ice in the Northern Hemisphere 1, Polar Geography, 24, 126 – 131, https://doi.org/10.1080/10889370009377692, 2000.

## **Editor**

Dear authors,

Thank you for detailed response to reviewers' comments. I have now read through your comments. Please go ahead and incorporate reviewers' comments in revising your manuscript as you have indicated in your response. Based on my reading, I may not send the revised manuscript back to reviewers for their second opinion.

I also have given your manuscript a thorough read and have some comments of my own. As you revise your manuscript please address following minor comments as well.

1) Please clarify if permafrost table is the same as the active layer depth or not.

Yes. In the UVic ESCM v2.10 model, the depth of the permafrost table corresponds to the active layer depth, which is defined as the shallowest depth at which the soil remains frozen for at least two consecutive years. We have clarified this point in the revised manuscript.

2) Your translucent colour plots (in response to reviewer #2) can go in supplementary information. Despite the overlaps, I found them helpful. It's your decision.

Thank you for your suggestion. We have included the translucent colour plots in the supplementary materials.

3) Please consider introducing your stabilization and overshoot scenarios briefly in the abstract to provide some context before delving into results.

Thank you for your detailed comments. We have provided a brief introduction of the stabilization and overshoot scenarios in the revised abstract to offer essential context.

4) In the abstract, when you say 4.5 to 6.5 million km2 of permafrost is lost, please also considering mentioning the model simulated pre-industrial permafrost extent for context.

Thanks. The model simulated pre-industrial permafrost extent is 17.01 million km<sup>2</sup>, and this information has been incorporated into the revised abstract to provide context for the projected permafrost loss.

5) Mention units of SPAW in the abstract.

Thanks. We have removed the abbreviation "SPAW" from the abstract to reduce the use of acronyms in the abstract. Its unit (million  $km^2$  °C<sup>-1</sup>) is now explicitly stated in the main text where the concept is first introduced.

6) Lines 62 and 63, clarifying the difference between response and feedback will be helpful.

Thank you for your suggestion. To clarify the distinction between response and feedback, we have revised "...how permafrost carbon response and feedback under temperature stabilization scenarios..." to "...how permafrost carbon will be released and further amplify global warming under temperature stabilization scenarios...".

7) If the model soil depth went down to say 40 m, will cryo-turbation spin up Yedoma. Likely not. Can you please add a sentence to make this clear?

Thank you for your suggestion. While the UVic ESCM v2.10 model resolves soil depth down to 250.3 m, it simulates both usual and permafrost soil carbon only within the top six layers, extending to a depth of 3.35 m. Consequently, cryo-turbation processes cannot initiate the formation of Yedoma under the current model configuration. We have included a clarification to make this aspect explicit in the revised manuscript.

8) Please note the size of pre-industrial usual and frozen soil C pools from your spin up.

Thanks. Under pre-industrial conditions, the simulated total soil carbon stock in the permafrost regions was 1031 [915 to 1149] PgC, of which 484 [383 to 590] PgC was classified as perennially frozen carbon and 547 [533 to 559] PgC was classified as usual soil carbon.

9) Since your runs aim to achieve a certain temperature threshold, your simulations are emissions-driven. Correct? Can you please make this explicitly clear? If correct, I am confused how does permafrost C emissions play a role. Does it change diagnosed emissions (Figure 1a)? But you mention increased radiative forcing due to permafrost C emissions which implies that it's the temperature that's changing. So does this mean you run your simulations with permafrost C feedback (PCF) turned on with emissions from the simulations without PCF. Did I miss this? If not, please clarify this.

Thank you for your suggestion. Our transient simulations are all driven by CO<sub>2</sub> emissions, whereas the spin-up simulations are conducted under fixed CO<sub>2</sub> concentrations at pre-industrial levels. For temperature stabilization and overshoot scenarios, the prescribed CO<sub>2</sub> emissions are derived from transient simulations with the permafrost carbon module deactivated, thereby excluding the influence of permafrost carbon emissions. Subsequently, these diagnosed CO<sub>2</sub> emissions are utilized to drive two sets of simulations, one with the permafrost carbon module activated and another with it deactivated. This setup enables us to isolate and quantify the additional warming and radiative forcing effects due to permafrost carbon emissions. We have clarified this procedure more explicitly in the revised manuscript.

10) Unless I missed this, can you please clarify how is permafrost is defined to be able to calculated permafrost extent?

The UVic ESCM v2.10 defines the total spatial coverage of permafrost as the area in which soil remains perennially frozen for a minimum of two consecutive years.

11) Please clarify what determines the boundary between usual and frozen soil C.

Thank you for your suggestion. In the UVic ESCM v2.10 model, usual soil carbon and permafrost carbon are depicted as two distinct depth-resolved carbon pools within the upper six soil layers. Soil carbon that is transported downward and crosses the permafrost table is transformed into permafrost carbon. Conversely, permafrost carbon that is moved upward and crosses the permafrost table is converted back into usual soil carbon. We have clarified this point in the revised manuscript.

## 12) Please introduce Figure 3 properly in the text and state its purpose.

Thank you for you suggestion. In the revised manuscript, we have added a proper introduction to the figure (originally Figure 3, now updated to Figure 4) to state its purpose and have adopted the same visual style as Figure 3 to enhance clarity and consistency. Specifically, Figure 4 illustrates how losses of permafrost area, permafrost carbon, and permafrost region soil carbon evolve relative to the SWL-1.5 scenario, providing a direct assessment of the reversibility of permafrost responses under both stabilization and overshoot scenarios. The updated Figure 4 is shown below.

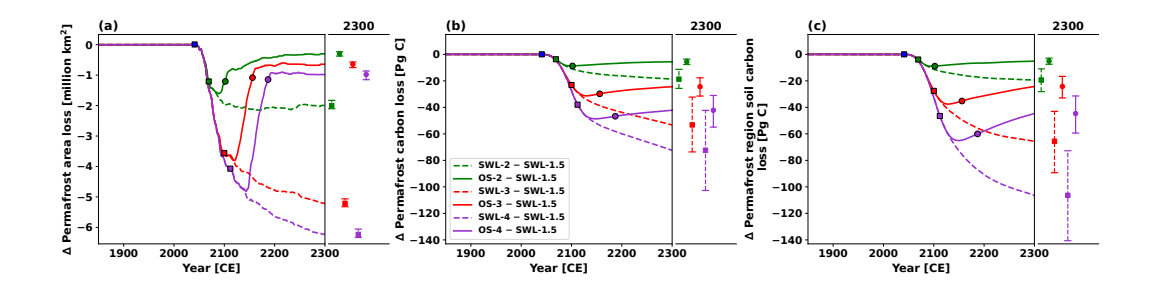
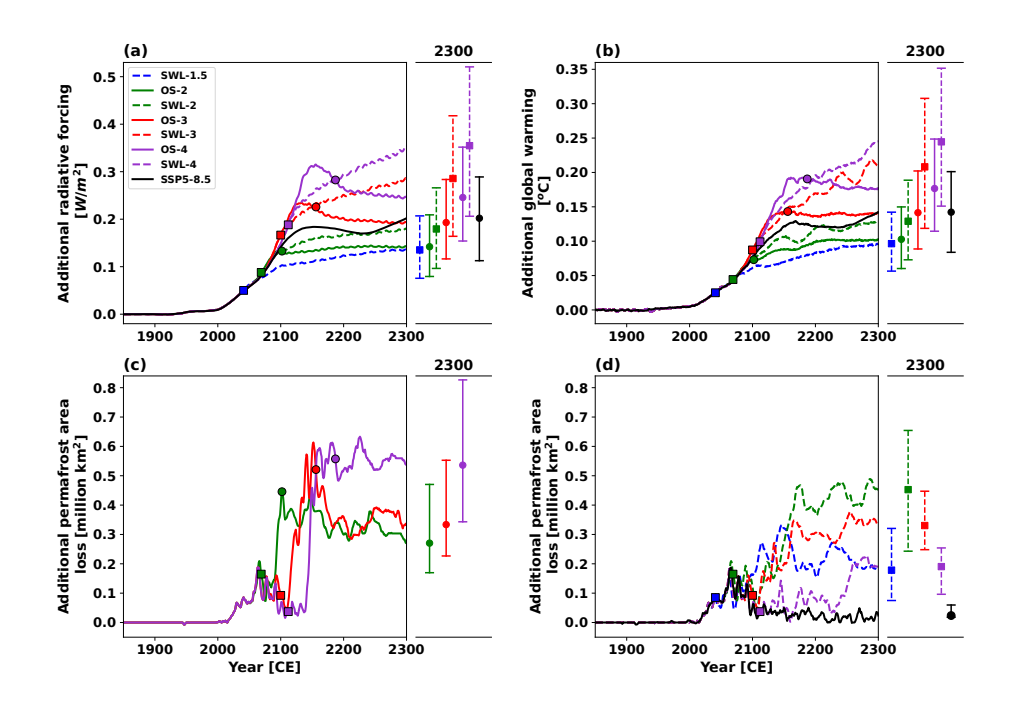


Figure 4. Similar to Figure 3, but showing timeseries of changes relative to the SWL-1.5 scenario in (a) permafrost area loss, (b) permafrost carbon loss, and (c) permafrost region soil carbon loss under stabilization and overshoot scenarios at 2.0 °C (green), 3.0 °C (red), and 4.0 °C (purple) global warming levels. Square markers indicate the time points when the temperature overshoot reaches its peak or stabilized warming begins, while circle markers indicate when the overshoot returns to 1.5 °C. Results represent the ensemble median of 250 simulations based on the PFC simulations. Dots on the right panels represent values in the year 2300, with uncertainty ranges estimated as the 5th to 95th percentiles.

13) In Figure 5, I found it hard to distinguish between filled squares and circles. Perhaps increase their size or put a black border around them.

Thank you for your suggestion. To improve visual clarity, we have increased the marker size and put a black border around them in the revised figure (originally Figure 5, now Figure 7). Similar improvements have also been applied to other relevant figures. The updated figure is shown below.



14) Line 351, "Permafrost C release significantly increase ...". Does "significantly" in this sentence means statistically significant? If not, try using some other word.

Thank you for your suggestion. To avoid confusion with statistical significance, we have replaced "significantly" with "evidently" in the revised sentence.

I look forward to reading a revised version of your manuscript.

Best regards, Vivek